PL-TR-97-3024

Direct Simulation Monte Carlo Modeling for Non-Equilibrium Flowfield Applications

D.C. Wadsworth
I.J. Wysong
D.H. Campbell

Raytheon STX Corporation
Air Force Research Laboratory
10 E. Saturn Blvd.
Edwards AFB CA 93524-7680

May 1999

Tasks 311 and 321 Final Report

AIR FORCE RESEARCH LABORATORY
AIR FORCE MATERIEL COMMAND
EDWARDS AIR FORCE BASE CA 93524-7048

NOTICE

When U.S. Government drawings, specifications, or other data are used for any purpose other than a definitely related Government procurement operation, the fact that the Government may have formulated, furnished, or in any way supplied the said drawings, specifications, or other data, is not to be regarded by implication or otherwise, or in any way licensing the holder or any other person or corporation, or conveying any rights or permission to manufacture, use or sell any patented invention that may be related thereto.

FOREWORD

This Final Technical Report was prepared by Raytheon STX Corporation (formerly Hughes STX), Edwards AFB, CA, under Tasks 311 and 321, Contract F04611-93-K-0005, for the Air Force Research Laboratory (formerly OL-AC Phillips Laboratory), Edwards AFB, CA. The project managers for AFRL/PRSA were David P. Weaver and Jay N. Levine.

This report has been reviewed and is approved for release and distribution in accordance with the distribution statement on the cover and on the SF Form 298.

CARL E. OUSLEY
Contracting Officer's Technical Representative

JAY N. LEVINE
Chief, Aerophysics Branch

PHILIP A. KESSEL
Technical Advisor
Propulsion Sciences & Advanced Concepts Division

RANNEY G. ADAMS III
Public Affairs Director

REPORT DOCUMENTATION PAGE

Form Approved
OMB No 0704-0188

1. AGENCY USE ONLY (LEAVE BLANK)	2. REPORT DATE	3. REPORT TYPE AND DATES COVERED
	May 1999	Tasks 311 & 321 Final Report, 1Nov93-30Sep96

4. TITLE AND SUBTITLE
Direct Simulation Monte Carlo Modeling for Non-Equilibrium Flowfield Applications

5. FUNDING NUMBERS
C: F04611-93-C-0005
PE: 62601F
PR/TA: 3058RF5C
PR/TA: 2308M19B
PR/TA: 3058RF9A

6. AUTHOR(S)
D.C. Wadsworth, I.J. Wysong, and D.H. Campbell

7. PERFORMING ORGANIZATION NAME(S) AND ADDRESS(ES)
Raytheon STX Corporation
Air Force Research Laboratory
10 E. Saturn Blvd.
Edwards AFB CA 93524-7680

8. PERFORMING ORGANIZATION REPORT NUMBER

9. SPONSORING/MONITORING AGENCY NAME(S) AND ADDRESS(ES)
Air Force Research Laboratory
AFRL/PRSA
10 E. Saturn Blvd.
Edwards AFB CA 93524-7680

10. SPONSORING/MONITORING AGENCY REPORT NUMBER
PL-TR-97-3024

11. SUPPLEMENTARY NOTES AFRL was formerly OL-AC Phillips Laboratory; Raytheon STX was formerly Hughes STX
The contract JON was 3058RF5C; Tasks 311 and 321 report the work done under JONs 2308M19B and 3058RF9A.
COSATI CODE(S):

12a. DISTRIBUTION/AVAILABILITY STATEMENT
Approved for public release; distribution is unlimited.

12b. DISTRIBUTION CODE
A

13. ABSTRACT (MAXIMUM 200 WORDS)

Questions important to modeling of nonequilibrium gas flows are examined. Testing and validation of Direct Simulation Monte Carlo (DSMC) codes have been performed. Several models for vibrational relaxation and chemical reaction of diatomic molecules have been implemented and studied parametrically, utilizing measurements and advanced calculations from the literature as benchmarks. DSMC results have been compared to rotational temperature measurements of nitrogen in finite background jet expansion flows. The influence of the rotational relaxation model, the influx boundary condition, and the outer boundary treatment on the simulation have been investigated.

14. SUBJECT TERMS
Direct Simulation Monte Carlo; DSMC; nonequilibrium flowfield; nonequilibrium gas flow; jet expansion flow; rotational relaxation model

15. NUMBER OF PAGES
56

16. PRICE CODE

17. SECURITY CLASSIFICATION OF REPORT	18. SECURITY CLASSIFICATION OF THIS PAGE	19. SECURITY CLASSIFICATION OF ABSTRACT	20. LIMITATION OF ABSTRACT
Unclassified	Unclassified	Unclassified	SAR

TABLE OF CONTENTS

LIST OF FIGURES

LIST OF TABLES

GLOSSARY
PARTS I, II and III

A	constant in Kafri and Levine model
Ar	argon
BL	Borgnakke Larsen
CVD	coupled vibration dissociation
D	dissociation energy
d	orifice diameter
DSMC	Direct Simulation Monte Carlo
EAE	exact available energy
E_v	vibrational energy
FHO	forced harmonic oscillator
GCE	generalized collision energy
GHS	generalized hard sphere
H	hydrogen
HCl	hydrogen chloride
He	helium
H_2	hydrogen molecule
I	iodine
ITFITS	Improvement to Forced Oscillator, Impulsive Transfer Semiclassical
k	Boltzmann constant
k_d	dissociation rate constant
LT	Landau-Teller
l	scale length
MW	Millikan and White
N	nitrogen
NO	nitric oxide
N_v	vibrational level population
N_2	nitrogen molecule
O	oxygen
O_2	oxygen molecule
P	collisional relaxation rate
P_o	stagnation pressure
P_∞	chamber background pressure
QCT	quasi-classical trajectory
STF	steric factor
TCE	total collision energy
T	temperature
T_o	stagnation temperature
T_r	rotational temperature (as used in Part III)
T_{rot}	rotational temperature (as used in Part II)
T_t	translational temperature (as used in Part III)

T_{trans}	translational temperature (as used in Part II)
T_v	vibrational temperature
T_{vib}	vibrational temperature (as used in Part II)
T_∞	chamber background temperature
VDF	vibrational distribution function
VFD	vibrationally favored dissociation
VHS	variable hard sphere
VSS	variable soft sphere
VT	vibrational-translational
WVB	weak vibrational bias
x	downstream distance from exit plane
Z	vibrational collision number
α	steepness parameter of the potential
ε	relative translational energy
φ	empirical exponent parameter
λ	constant in maximum entropy model
λ	parameter indicating degree of vibrational favoring (as used in Part II)\
Θ_v	characteristic vibrational temperature
σ_d	dissociation cross section
σ_{el}	elastic collision cross section
σ^o	state specific cross section
τ_{inc}	incubation time
τ_v	vibrational relaxation time

SUMMARY

The goal of this project was to improve and validate modeling tools for nonequilibrium gas flows. Such flows are key in many practical problems such as shock layer radiation and surface heating of atmospheric re-entry vehicles and spacecraft, rocket plume core radiation and plume/freestream interaction, electric propulsion thrusters, and low-pressure plasma-processing reactor design. Predicting the important physics of these gas flows requires the ability to model individual molecular collisions and simulate the energy transfer and chemical processes in a computationally efficient manner. The most widely used technique for simulating gas flows through computing individual collisions is known as Direct Simulation Monte Carlo (DSMC). This project has produced several DSMC codes for in-house simulations of immediate interest. In addition, this project has undertaken several studies that address the sensitivity of DSMC results to the various simplified energy transfer and chemistry models that are commonly utilized.

The first part of this report presents the results of an investigation into the use of shock tube measurements of reaction rate constants and induction times to validate models of vibrational relaxation and dissociation. Several DSMC vibrational energy transfer models are examined. It is concluded that the strong coupling of vibrational transfer and dissociation in a shock tube precludes using the results to validate the model for one of these processes without having data on the other. In addition, an investigation of vibrational favoring in air exchange reactions is performed, and it is shown that room temperature vibrational disposal measurements of the reverse (exothermic) reactions provide sufficient information to conclude that vibrational favoring is not important in these cases.

The second part of this report looks in more detail at various DSMC models that can be used to simulate molecular dissociation. It is shown that reproducing a temperature-dependent rate constant (Arrhenius-type) is an insufficient validation for the model to reasonably reproduce far-from-equilibrium reacting flows. In the absence of state-specific data, quasi-classical trajectory (QCT) results for H_2 dissociation are used to compare the qualitative behavior of different models in terms of vibrational favoring.

In the third part of the report, direct simulation Monte Carlo simulation results are compared to rotational temperature measurements of nitrogen in finite background jet expansion flows. The influence of the rotational relaxation model, the influx boundary condition, and the outer boundary treatment on the simulation are shown to have a significant effect on the predicted rotational temperate shock structure.

A number of details necessary for the proper DSMC implementation of collision-selection models, rotational transfer, vibrational transfer, and chemistry have been worked out and are given in the appendix.

PART I: INFLUENCE OF VIBRATIONAL NONEQUILIBRIUM ON CHEMICALLY REACTING RAREFIED FLOWS: TOWARD EXPERIMENTAL VERIFICATION OF DSMC MODELS

INTRODUCTION

An accurate model of chemical reactions is a key factor in obtaining useful predictions of radiation and surface heating around re-entry vehicles or spacecraft and in understanding plasma processing environments, etc. These types of flows, however, typically display significant thermal and chemical nonequilibrium. For instance, the vibrational temperature of the molecules may often be substantially different than the translational temperature of the gas. Indeed, molecules in these flows often have a non-Boltzmann vibrational state distribution such that there is no true temperature associated with the vibrational degrees of freedom. At the same time, the degree of population of high vibrational levels is often the controlling factor in the probability of dissociation and endoergic exchange reactions. Recent work by Boyd, *et al.*[1] uses Direct Simulation Monte Carlo (DSMC) to predict density and temperature of NO produced in a re-entry bow shock and shows that different nonequilibrium chemistry models can change the predicted number density of NO, and thus the predicted ultraviolet radiation, dramatically. Thus, it is clear that an accurate model for chemical reactions under conditions of vibrational nonequilibrium is needed, and extensive research in this area has taken place over the past several decades.

DSMC calculations, which simulate individual gas particle collisions, are well suited to the inclusion of physically accurate chemistry models that are based on the translational and internal energy states of each molecule. Nonequilibrium chemistry models have been the topic of considerable research. Various models and approximations are being implemented in DSMC codes for use in predicting rarefied flowfields. One could be certain that a DSMC chemistry model is accurate for any flowfield if one had a complete set of state-specific reaction and energy transfer cross sections as a function of collision parameters (velocity, impact parameter, etc.) for all species. Future high-level calculations and laboratory measurements may ultimately provide these, but in the meantime, cruder means of model validation are sought. Experimental data against which to compare nonequilibrium chemistry models, however, are quite difficult to obtain. Large shock tube facilities are one way to try to create high-temperature nonequilibrium gas flowfields, but detailed molecular data from these flows are rare.

Preliminary consideration by this group of possible experiments that couple rarefied flowfields and chemical reactions revealed the necessity for a series of parametric calculational studies to clarify what data will be useful. Many measurements of reacting flowfields or state-specific chemical reactions would be possible that would not increase the understanding of how to properly implement a general DSMC chemistry code or distinguish between some of the candidate models. For instance, Treanor, *et al.*[2] have shown that unless the degree of thermal nonequilibrium in an air shock is great (vibrational temperature is less than one-tenth the translational temperature), then differences between the predictions of different chemistry models on the production of NO (which is the measured quantity in some shock tube experiments) cannot be distinguished.

Shocked gas flows are typical of many nonequilibrium flows in that the translational and rotational degrees of freedom very quickly reach some high temperature, while the vibrational degrees of freedom lag behind with a much lower energy. Because this is the key feature of the nonequilibrium chemistry of many rarefied flows, it is possible to perform useful parametric calculational studies for a highly simplified case. The temporal evolution of initially vibrationally cold molecules in an isothermal bath (described in more detail here) that is in translation-rotation equilibrium displays many of the same physical mechanisms that control the nonequilibrium chemistry of shocked gas flows.

ATOM EXCHANGE REACTIONS

A wide variety of exoergic atom exchange reactions are known to produce products that are highly vibrationally (or rotationally) excited, or "hot," compared with a thermal or statistical distribution of the available reaction energy into all degrees of freedom. Levine, *et al.*[3,4] have shown that the principle of detailed balance requires those reactions that produce enhanced post-reaction vibrational excitation in the exoergic direction must also have their reaction probability enhanced by vibrational excitation of reactants in the reverse (endoergic) direction. This characteristic will be referred to as "vibrational favoring." Note that any endoergic reaction will be enhanced by vibrational excitation, merely because the amount of total energy available in the collision is increased (assuming that all types of energy contribute to the activation energy). "Vibrational favoring" refers to an increase in reaction probability beyond what would be expected due to the amount of total energy available and indicates that vibrational energy is more effective than other types of energy in promoting reaction.

The works of Levine, *et al.* describe in detail a compact method to quantify the enhancement of chemical reactions due to reactant internal energy using a single parameter, λ. When $\lambda = 0$, then there is no vibrational favoring, and the reaction probability is increased by all types of energy equally. This is known as the "prior" case and reflects the statistically most likely situation in the absence of any constraint and, therefore, the maximum entropy case. A discussion of this approach, as applied to DSMC, may be found in Marriott[5] and Gallis.[6] A large negative value of λ indicates that the reaction is strongly vibrationally favored. It has been shown that many exchange reactions, especially of hydrogen and halogen-bearing species, are highly vibrationally favored, while some others show no such favoring.

For air chemistry, the two Zel'dovich atom exchange reactions are important:

$$N2(v) + O \leftrightarrow NO + N \tag{1}$$

$$NO(v) + O \leftrightarrow O_2 + N \tag{2}$$

For each of these reactions (exothermic direction, $\leftarrow$), a measurement of vibrational energy disposal to the products is available[7,8] at room temperature, in both cases showing a nearly statistical distribution. Detailed balance then dictates that in the endothermic direction ($\rightarrow$) these two reactions are not (or are weakly) vibrationally favored. Recent quasi-classical trajectories (QCT) calculations[9] of state-to-state reaction cross sections for Reaction (1) provide valuable detailed information, yet also confirm this qualitative conclusion. The QCT results show that, for a given translational and rotational temperature, the reduction in reaction rate constant due to decreasing vibrational temperature of the reactants is about what would be expected for a case with a slight vibrational favoring of about $\lambda = -2$. Thus, traditional rarefied flow data are not the only source for validation of nonequilibrium chemistry models. In the case of the Zel'dovich reactions, literature results on the vibrational excitation of products for the reverse reactions provide a valuable test of the degree of vibrational favoring of the forward reactions.

DISSOCIATION

Collision-induced dissociation reactions of diatomic molecules are often considered to be vibrationally favored, yet unambiguous information on the degree of favoring is scant. Since dissociation reactions under conditions of significant vibrational nonequilibrium can be the controlling chemical step in the systems mentioned here in the introduction, an ability to model these reactions with the correct amount of vibrational favoring is needed.

The state-specific cross sections for the dissociation of $H_2(v)$ colliding with argon have been calculated[11] using QCT. For this case the vibrational favoring for this reaction is quite strong, corresponding to λ of approximately -12, but H_2, with its very widely spaced vibrational and rotational levels, is not necessarily a good model for other diatomic species. A molecular beam study of $H_2^+(v)$ dissociating on collision with He also showed a strong vibrational favoring[12], reflecting a λ of about -8. Several state-specific cross sections for the dissociation of H_2 colliding with H have been calculated using QCT;[13] the results demonstrate a strong enhancement of dissociation probability by internal energy, especially vibrational energy. Unfortunately, neither state-specific dissociation measurements nor QCT calculations are available for O_2 and N_2. Instead, some shock tube data on the nonequilibrium dissociation rate coefficient and incubation time have been obtained for these species, and a number of studies have attempted to deduce information on the degree of vibrational favoring based on the these macroscopic quantities.

It has long been recognized that vibrational relaxation and dissociation processes are fully coupled in shocks and other rarefied gas flows. Even without any vibrational favoring, dissociation will always occur more rapidly from molecules at higher vibrational levels compared with molecules at lower vibrational levels. This is because of the much greater amount of total energy available in the collision if the two molecules have the same translation/rotation temperature or energy. So, the dissociation process is constantly removing high v (vibrational level) molecules and driving the gas away from a Boltzmann distribution of vibrational energy, while vibration-to-translation (VT) relaxation is constantly reshuffling the vibrational distribution function (VDF) toward a Boltzmann distribution. The competition between these processes is known as coupled vibration dissociation (CVD) and is what determines the k_d^*, the quasi-steady nonequilibrium dissociation rate constant that is observed in shocks and is reduced from the equilibrium value of k_d^{eq}. An approximate value of $p\tau_d$, where p is pressure and τ_d is an approximate characteristic time for dissociation, is included in Figure 1, which illustrates that, for O_2-argon, CVD is important at temperatures above about 4000 K, where τ_d and τ_V (the vibrational relaxation time) become of comparable magnitude. Therefore, any model of a shock tube dissociation measurement must include information on, or assumptions about, both the state-specific dissociation cross sections and the state-specific vibrational relaxation cross sections. A number of studies have addressed this problem and many have modeled shock tube dissociation data using various dissociation and vibrational relaxation models.[14,18-25]

VIBRATIONAL RELAXATION SIMULATIONS

The case chosen for these studies is O_2 in an isothermal heat bath of argon. This has been the subject of a number of previous modeling studies,[18-23] primarily because of its simplicity and the availability of experimental shock tube measurements of k_d^* and incubation time for this case over a range of temperatures by Wray[26] and Camac and Vaughan.[27] The molecules have the translational and rotational degrees of freedom in equilibrium at some temperature T, but at time $\tau = 0$, the molecules have a vibrational temperature (Boltzmann distribution) of 200 K. The O_2 is considered to be very dilute so that the bath temperature, T, remains constant and O_2-O_2 collisions may be neglected. In this way, studies of the effect of the key features of CVD can be performed in a very simplified context. All simulations presented here have used T(bath) = 7000 K.

The code used here follows the basic methodology of Bird.[28] The relaxation logic is based on the Particle-Selection Prohibiting Multiple Relaxation method of Haas, *et al.*[29] More complete discussion of the current code will be given in Wadsworth's "Comparison of Vibration-Translation Models for DSMC Method."[†] For the O_2-argon isothermal bath of interest, one needs only to consider collision events involving one O_2 molecule with one argon atom, with

[†] Wadsworth, D.C., Raytheon STX, AFRL, Edwards AFB, CA, In preparation.

only O_2 dissociation and O_2 vibrational relaxation events being allowed. For consistency, collision parameters for O_2 with argon are based on the variable soft sphere (VSS) values given by Koura.[30] The O_2 vibration levels are based on the bounded, quantized, simple harmonic oscillator model, with a vibrational temperature Θ_V = 2274 K, yielding 27 bound vibrational levels. The various models of dissociation and VT exchange are implemented into the basic code with only minor changes to the collision logic.

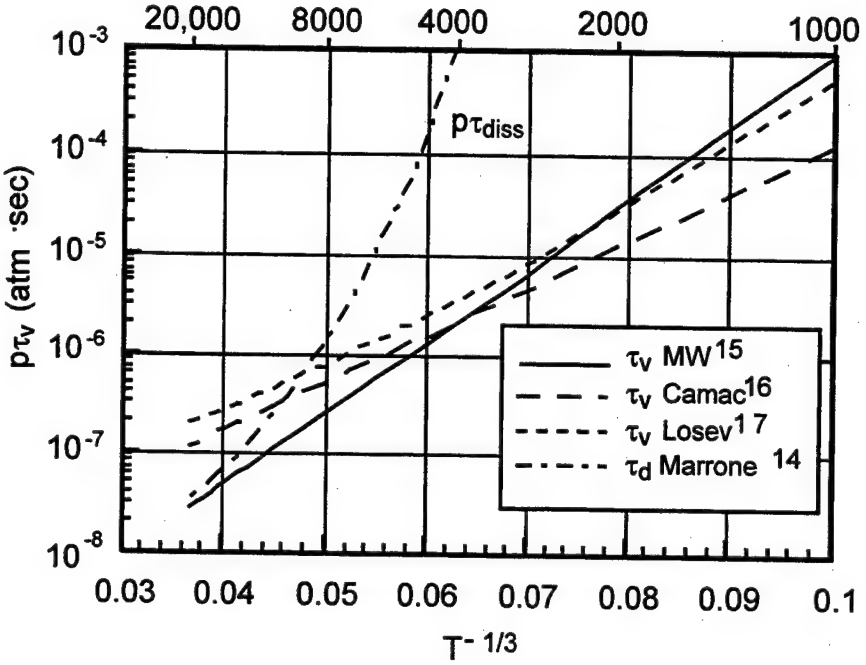

Figure 1
Predicted Correlation of $p\tau_V$ with Temperature for O_2-argon from Various Sources
An approximate value of $p\tau_d$ (average time to dissociation) is included for comparison

It is worth stating that the only calibration used for many VT models is that of matching the overall vibrational relaxation time (τ_V) of the gas at a given temperature or range of temperatures to that predicted by a measured correlation. Three such correlations for O_2-argon collisions found in the literature are shown in Figure 1. The correlation of Camac[16] is based on data which extend from 1200 to 5000 K. The correlation of Millikan-White[15] (MW) is based on data from White and Millikan[31] from 1000 to 3000 K as well as the data of Camac. The correlation of Losev[17] is based on data from 4000 to 10,000 K as well as previous data. Unfortunately, the validity of extrapolating any correlation to higher temperatures is questionable. In addition, the assumptions of the Landau-Teller model (harmonic oscillator, only Δv = 1, Boltzmann vibrational distribution), which are used to reduce shock data to obtain a value for τ_V, begin to break down at T > 2000 K. Thus, a correct value for τ_V is problematic and will be seen to have an effect on k_d*.

The various methods of modeling VT transfer that have been incorporated into the DSMC code are described here briefly. Model I is the Borgnakke-Larsen (BL) method,[32] which simulates VT relaxation by allowing a change in vibrational state (or energy) every Z collisions. Here, Z is the vibrational collision number, based on the translation-rotation temperature of the gas so that the overall relaxation time τ_V matches the "known" experimental value. When a collision is permitted to undergo VT relaxation, the post-collision state (or energy) of the O_2

molecule is sampled from an equilibrium distribution based on equipartition of the sum of translational and vibrational energy of the collision among the available modes.

In contrast to the BL model, one may dispense with Z and simulate VT transfer using state-to-state transition probabilities. This was first implemented for DSMC by Boyd[33] and later by Abe,[34] who formulated probabilities for $\Delta v = 1$ transitions as a function of collision velocity and initial vibrational level in such as way as to reproduce the correlation between τ_V and gas temperature. It seems that, as the gas temperature increases, the velocity-dependent transition probabilities in this model do not produce equipartition of energy, due to approximations made in the derivations (see Choquet[35]). However, for the case of a thermal bath, the velocity-dependent probability is not really needed. Abe[34] has presented a model with constant transition probability for each vibrational level (independent of collision energy). (Note Abe's Equation 32 in Reference 34 is valid for hard sphere only). This will correctly equipartition energy and can be set to produce the desired value of τ_V, except at very high temperatures, where probabilities for high v states exceed unity and where multi-quantum transitions are important. This model has been labeled as Model II.

A third model for VT transfer used in this study is that first presented by Koura[21,36] for Monte Carlo implementation. The probability equations are given in Heidrich, *et al.*,[37] who referred to it as Improvement to Forced Oscillator, Impulsive Transfer Semiclassical (ITFITS). It is based on the forced harmonic oscillator approximation (FHO), as originally derived by Kerner[38] and Treanor,[39] and includes multi-quantum VT transfer. Koura implements the cross section (as a function of relative velocity and initial vibrational level) for VT transfer for a diatom colliding with an atom in his Monte Carlo simulations of O_2-argon. The same expression (in a slightly different form) for VT probabilities was presented by Adamovich, *et al.*[40] who use the probabilities to compute state-specific rate coefficients for vibrational transfer. The work by Adamovich, *et al.* also presents the formulas for probability of vibration-vibration transfer and the resulting rate coefficients. It includes an extensive validation of the FHO model by comparing the results for N_2-N_2 and O_2-O_2 relaxation rate constants with semi-classical 3-D trajectory results by Billing[41,42] over a range of temperatures and vibrational levels. In addition, the value of τ_V predicted by FHO for N_2- N_2 and O_2-argon is shown to be in reasonable agreement with measured values over a range of temperatures.

The FHO or ITFITS model has two adjustable parameters, the steepness parameter of the potential, α, and a steric factor (STF). For O_2-argon, Koura estimates the values of α and STF that result in exact agreement with the MW estimation of τ_V in the range 300-2000 K, but diverges at $T > 2000$ K. The ITFITS model for VT transfer has been implemented in the DSMC code using the value recommended by Koura for α and STF and will be called Model III.

Some results of heat bath calculations for O_2-argon using the three VT models are presented in Figures 2 and 3. The mean vibrational energy of a gas may be defined as:

$$\langle v \rangle = \frac{\sum_v E_v N_v}{\sum_v N_v} \tag{3}$$

where E_V is the energy of each vibrational level (assuming that the ground level has $E_V = 0$), and N_V is the number of molecules that populate that vibrational level. Figure 2 shows several examples of $\langle v \rangle$ versus time in the heat bath, demonstrating that, in the absence of dissociation, all VT models used in this study achieve the correct equilibrium value of $\langle v \rangle$, but vary in the length of the relaxation time. The shape of all the curves in Figure 2 follows that predicted (not shown) by the Landau-Teller (LT) equation: $d\langle v \rangle/dt = (\langle v \rangle^{eq} - \langle v \rangle)/\tau_V$ (note that this equation

provides the definition of τ_V). Here, $\langle v \rangle^{eq}$ is the equilibrium mean vibrational energy at the heat bath temperature. Since the various VT models reproduce the shape of the LT equation, the overall vibrational relaxation predicted by any model may be approximated by some value of τ_V that causes the LT equation to match the plot of $\langle v \rangle$ versus time. Figure 2 demonstrates the range of uncertainty in τ_V at 7000 K.

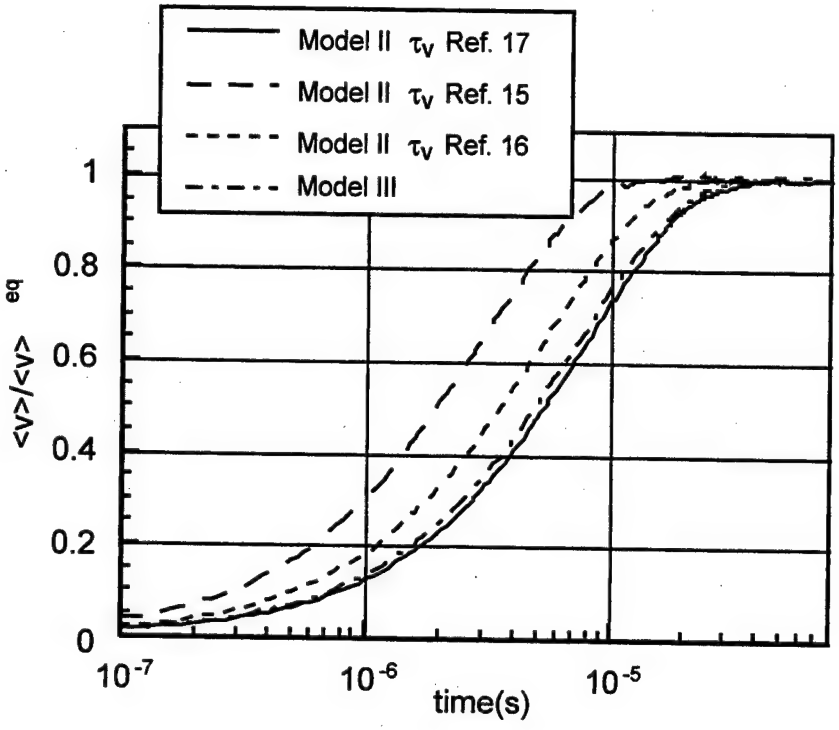

Figure 2
Relaxation of the Mean Vibrational Energy in the Isothermal Bath
The results using Model I are not shown, since for each value of τ_v, the curve for Model I lies on top of the curve for Model II

When Models I and II use the same value of τ_v, the relaxation of $\langle v \rangle$ versus time is the same. Yet, at short times, the actual VDFs produced by Models I and II can differ substantially. Figure 3 demonstrates a simulation using Model I and Model II with the same value of τ_v. Figure 3(a) shows the resulting VDFs at an early time during the vibrational relaxation, $t \approx 0.1*\tau_v$. (The MW value for τ_v is used in this case). Assuming that Model II is closer to reality, the result of Model I shows a systematic bias in VDF in the short time (few collision) regime. One can see by comparison with the line showing a Boltzmann VDF for 7000 K how Model I creates a bimodal VDF. Those collisions that are allowed to undergo vibrational relaxation immediately jump to the VDF of the bath.

One may define a "vibrational temperature," T_v, by:

$$\langle v \rangle = \frac{\sum_v E_v \exp(-E_v / kT_v)}{\sum_v \exp(-E_v / kT_v)} \tag{4}$$

(where k is Boltzmann's constant), and solving for T_v based on the value of at $\langle v \rangle$ any point in time. Figure 3(b) shows that, based on this definition, the T_v produced by the two models follows the same progression in time. However, if T_v is defined as:

$$T_v = \frac{\Theta_v}{\ln(N_0 / N_1)} \tag{5}$$

as is often the case (where N_0 is the population in v = 0 and N_1 is the population in v = 1), Figure 3(c) shows that Model I produces a different value of T_v compared with Model II at short times, due to the differences in VDF. It must be emphasized at this point that a gas whose VDF does not follow a Boltzmann distribution does not have a well-defined vibrational temperature, and any presentation of an approximate T_v of such a gas is not meaningful without an accompanying statement of how the approximate T_v is defined. The systematic bias of the BL model complicates any attempt at quantitative comparisons between results in the literature of T_v.

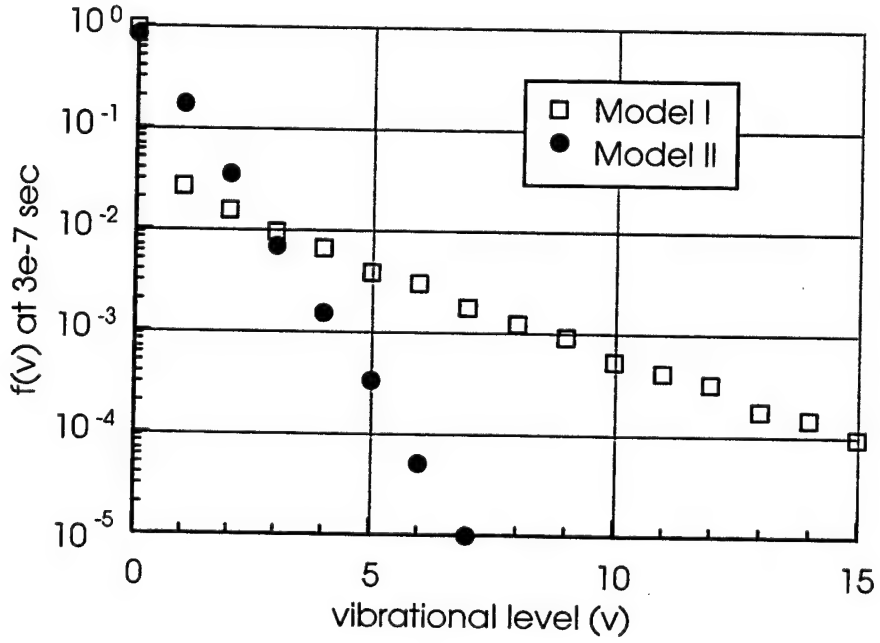

Figure 3(a)
Vibrational Distribution Function Predicted by Model I and Model II at t = 0.1*τ_v (using τ_v MW)

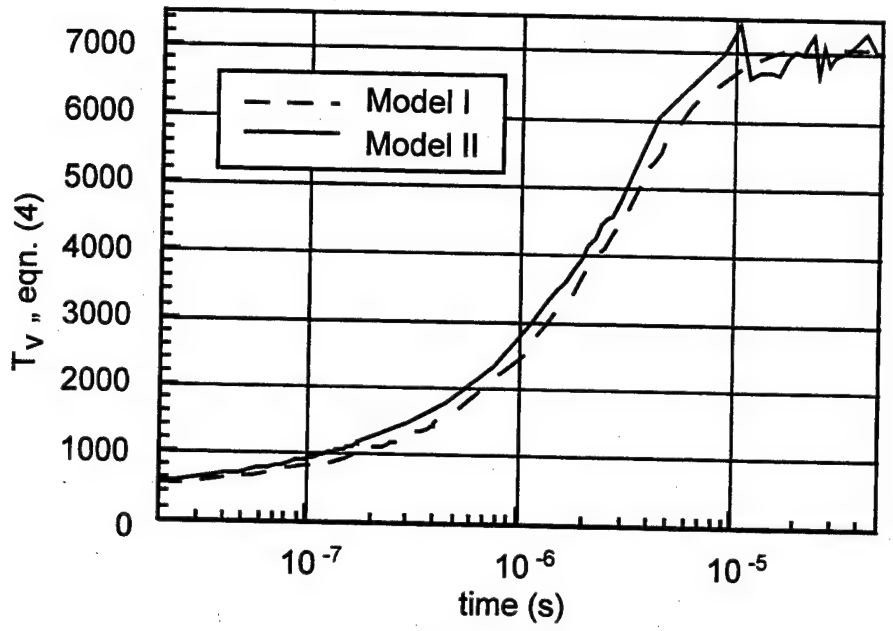

Figure 3(b)
Vibrational Temperature as a Function of Time using Equation (4) for Model I and Model II

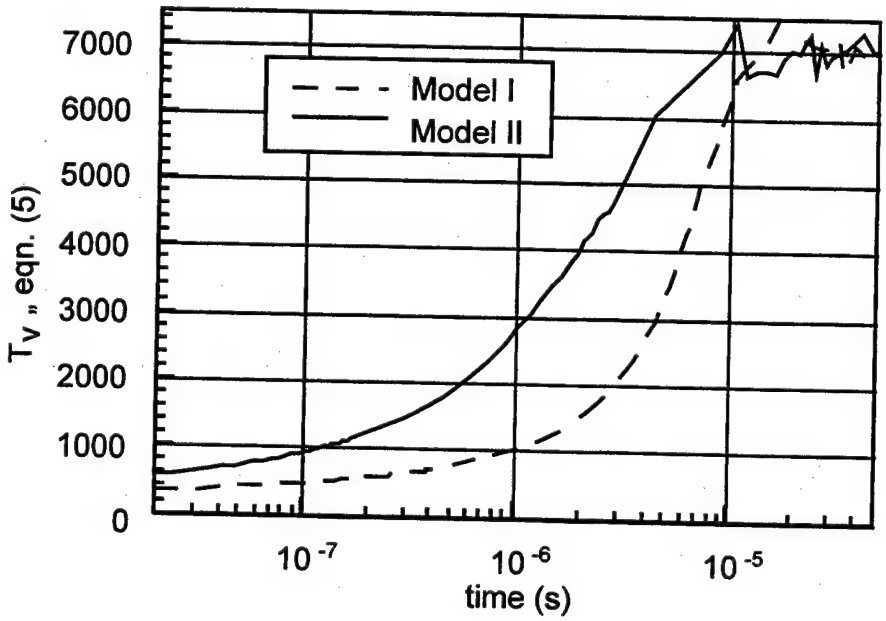

Figure 3(c)
Vibrational Temperature as a Function of Time using Equation (5) for Model I and Model II

INTRODUCTION OF DSMC DISSOCIATION MODELS

As discussed in the previous section, many methods for modeling dissociation of diatomics have been presented in the past. The number of methods that have been used in the context of DSMC simulations is more limited. The method introduced by Bird[43] to simulate chemical reactions in DSMC calculations is widely utilized. It expresses the probability of dissociation as a function of the total collision energy (TCE) and uses adjustable parameters to reproduce measured dissociation rate coefficients as a function of temperature under equilibrium conditions. Recently, Bird introduced a different DSMC method for chemical reactions,[28,44,45] known as the exact available energy (EAE) approach. It performs a BL vibrational redistribution on every collision that has sufficient energy to dissociate and, using "notional" vibrational levels that extend above the dissociation energy (D), chooses a post-collision level based on the total pre-collision energy. If the post-collision level is above D, then a dissociation reaction is assumed to have taken place. Under equilibrium conditions, this method has been shown to reproduce fairly closely the measured dissociation rates for O_2-O_2 and N_2-N_2 as a function of temperature. Like the TCE method, the EAE is based on the total energy of a collision, with no favoring of vibrational energy. The EAE dissociation model has been implemented in the DSMC code. More details are provided in Reference 46. Figure 4 shows the equilibrium dissociation rate coefficient predicted by the EAE model for O_2-argon collisions.

Haas and Boyd[20] introduced the vibrationally favored dissociation (VFD) model which modifies the TCE model and allows for favoring of vibrational energy in the dissociation probability through an adjustable (empirical) parameter, ϕ. Hash and Hassan[47] have proposed a modified version of the VFD model where the value of ϕ is determined without experimental input. Ivanov, *et al.*,[48] have implemented a dissociation model in their DSMC code that uses probabilities based on state-specific rate constants (as formulated by Warnatz[49]) that include a certain (fixed) amount of vibrational favoring. Macheret and Rich[18] have presented a threshold line model to obtain dissociation rate coefficients for given (unequal) translation/rotation and vibrational temperatures. Recently, Boyd[50] has adapted this model for a DSMC implementation, using one probability expression for dissociation from high vibrational levels and a different (reduced) probability expression for low vibrational levels. The reduction in probability for lower levels means that this model is vibrationally favored. The probabilities include a single adjustable STF for calibrating the results for equilibrium against measured rate constants.

An approach to modeling vibrationally favored dissociation based on the formalism of Levine[4] (as discussed above for exchange reactions) was used by Kiefer,[19] Gonzales,[22,23] and Shizgal[24] for continuum simulations of nonequilibrium gases. For particle simulations, Marriott,[5] Gallis,[6] and Koura[21] have presented adaptations of the Levine approach; all of these include an adjustable parameter, λ, that indicates the degree of vibrational favoring, but is formulated in different ways. The concept for a Monte Carlo implementation is to have a prior state-specific cross section, σ^0, that reflects the probability for dissociation from a given level as a function of translational energy. The prior cross section is intended to express the probability with no constraint (such as vibrational favoring) and thus the condition of "maximum entropy." Then the prior cross section is multiplied by a factor $\exp(-\lambda f(E_V, E_{tot}))$ to simulate the constraint of vibrational favoring, where f(v) is related to the fraction of collision energy that is in the vibrational mode. (Note that there is a sign change between Levine's papers and some of the more recent formulations. Originally, the formulas were such that a negative value of λ represented vibrational favoring. Some recent versions, including Koura's and References 19 and 22-24 have changed the sign such that a positive value of λ represents vibrational favoring.) Unfortunately, the prior cross section for a dissociation reaction (which in principle comes from counting possible post-reaction states) is dependent on the intermolecular potential that is assumed[53] and a general expression is not known. Kafri and Levine[54] have suggested one approximation as $\sigma^0 = A(E-D)^2/(Et)^{1/2}$.

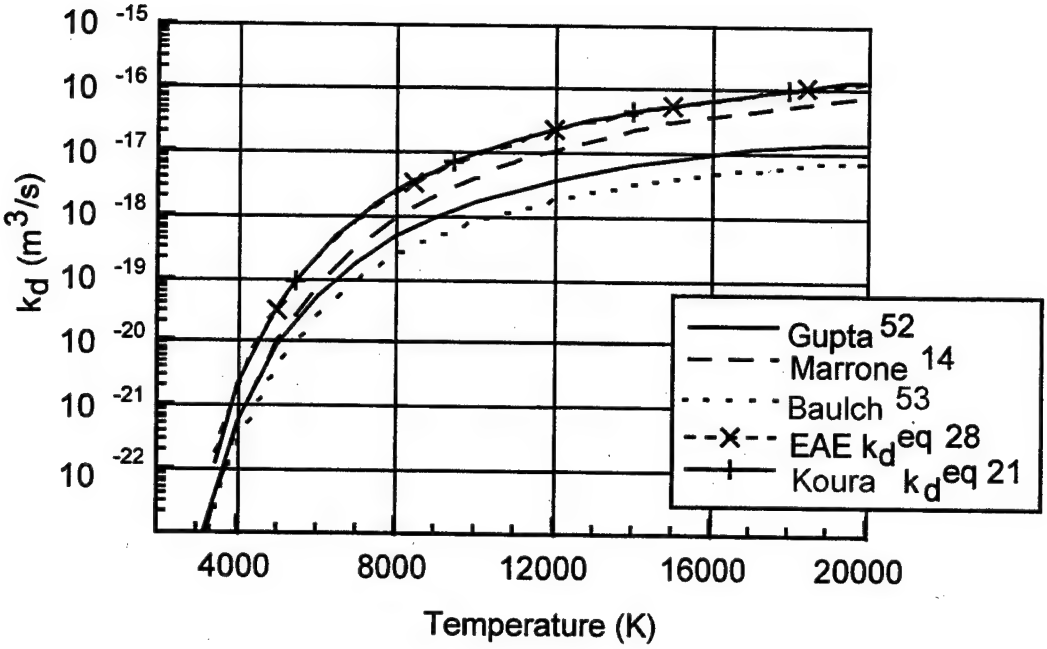

Figure 4
Rate Constants for Dissociation of O_2 by Argon
The DSMC results represent true equilibrium rate constants (the VDF of the molecules in the simulation is constrained to $T_v = T$). The Marrone value (Equation 7), as explained in the text, is estimated for true equilibrium, and the Gupta value (Equation 8) and Baulch value (Equation 9) are based on experimental measurements that reflect some nonequilibrium

Although the continuum versions mentioned above (References 19, 22-24) make use of the Kafri and Levine[54] suggestion for the prior cross section, which includes the total collision energy, Koura[21] uses a different expression, $\sigma^0 = \sigma_{el}(1-(D-E_V)/\varepsilon)$. Here σ_{el} is the elastic collision cross section based on the symmetrized relative collision velocity, E_V is the vibrational energy, and ε is the relative translational energy. This prior cross section does not include any contribution to dissociation probability from rotational energy, which may not be physically realistic for some cases. The full expression for dissociation cross section used by Koura is:

$$\sigma_d = \sigma_{el}(1-(D-E_V)/\varepsilon)STF \exp[\lambda(E_V/D - 1)] \quad \text{for } \varepsilon>(D-E_V) \tag{6}$$

and $\sigma_d = 0$ otherwise. Koura recommends STF = 1 and $\lambda = 2$ for O_2-argon. In the DSMC code used for the present parametric studies, this expression has been implemented. The STF was set equal to one for the prior case ($\lambda = 0$). When the value of λ is changed, however, the value of the STF was adjusted accordingly so that the degree of vibrational favoring does not change the equilibrium dissociation rate constant. For instance, when $\lambda = 2$, the STF = 2.4. Since Koura always uses STF = 1, his k_d^{eq} will be lower than this one for $\lambda = 2$. As shown in Figure 4, under equilibrium calculations the rate constant predicted by the Koura model for O_2-argon and that from the EAE model are virtually identical, but, as seen below, the rate constant predicted under nonequilibrium (shock tube) conditions by the Koura model, even for the $\lambda = 0$ (prior) case, is lower than that of the EAE model. This may be because Koura's expression for the prior cross section is not truly representative of the maximum entropy case.

DISSOCIATION SIMULATION RESULTS

Ideally, one would like to validate a nonequilibrium dissociation model in the following steps. First, ensure that the model predicts the correct rate constant under fully equilibrium conditions. Then, compare the model predictions for the quasi-steady (nonequilibrium) dissociation rate constant and incubation time in a shock with measured values. Unfortunately, both of these steps are far from straightforward. The various literature measurements of the dissociation rate constant for a given system (O_2-argon is used here) show a considerable amount of scatter, which tends to increase at higher temperatures. In addition, most of these measured values are from gases with varying amounts of nonequilibrium, and thus do not truly measure the equilibrium rate constant. Marrone and Treanor[14] have stated that vibrational nonequilibrium introduces the pre-exponential temperature dependence in the Arrhenius expression for the dissociation rate constant, and recommended

$$k_d^{eq} = 9e14*\exp(-59380/T)\ cm^3/mole*s \tag{7}$$

as the equilibrium rate constant expression for O_2-argon. This expression agrees with the shock tube observations of Camac and Vaughan[27] up to 4000 K, but at higher temperatures diverges as the shock tube data reflect the effect of nonequilibrium as the characteristic time for dissociation becomes comparable to τ_v. Kondratiev and Nikitin[55] have stated that the rate coefficient for CVD will be proportional to exp(-D/kT) in the low temperature limit and proportional to T^{-1}exp(-D/kT) in the high temperature limit. Haas and Boyd[20] have adopted the above expression recommended by Marrone to calibrate their VFD model for the equilibrium case.

It should be noted that the two dissociation models employed in this study do not use adjustable parameters to set the equilibrium rate constant, although an STF could be added to reduce the predicted rate constant, if desired. It happens that the two models produce nearly identical equilibrium rate constants for O_2-argon, as shown in Figure 4. Both are a factor of 2-3 higher than the Marrone recommendation, and up to a factor of 10 higher than the expression recommended by Gupta[51]:

$$k_d = 3.61e18*T^{-1.0}\exp(-59400/T)\ cm^3/mole*s \tag{8}$$

or Baulch[52]:

$$k_d = 1.80e18*T^{-1.0}\exp(-59380/T)\ cm^3/mole*s \tag{9}$$

Both the Gupta and Baulch recommendations are based on all available measurements and presumably reflect the effects of nonequilibrium at temperatures above 4000 K. However, the Baulch recommendation is a factor of 2 lower than Marrone's[14] in the 3000-4000 K range. Also, more recent shock tube data by Jerig *et al.*[56] fit the O_2-argon dissociation rate constant for the range 2400 to 4100 K to:

$$k_d = 1.6e18*T^{-1.0}\exp(-59380/T)\ cm^3/mole*s \tag{10}$$

almost identical to the Baulch recommendation. Thus, the proper value for k_d^{eq} to match the DSMC model to is ambiguous.

The second step of the validation – comparing nonequilibrium rate constants with shock measurements, is complicated by the influence of vibrational relaxation, as previously discussed. Figures 5(a) and 5(b) show parametric studies to illustrate the effects of various assumptions on the results of shock tube simulations. The number of O_2 molecules in the simulation cell is shown as a function of time in a semilog plot. The slope of the linear (quasi-steady) portion

yields the value of k_d * for each simulation. The intercept of the extrapolated line with a horizontal line at $n(O_2) = 1$ gives the value of τ_{inc}, (the incubation time). Figure 5(a) shows how the VT model affects the simulation result for k_d *. Even if the dissociation model is identical (the EAE model is used for both cases shown in the figure), using a VT model (Model II is used here) that has a different effective τ_V will result in a difference in k_d *.

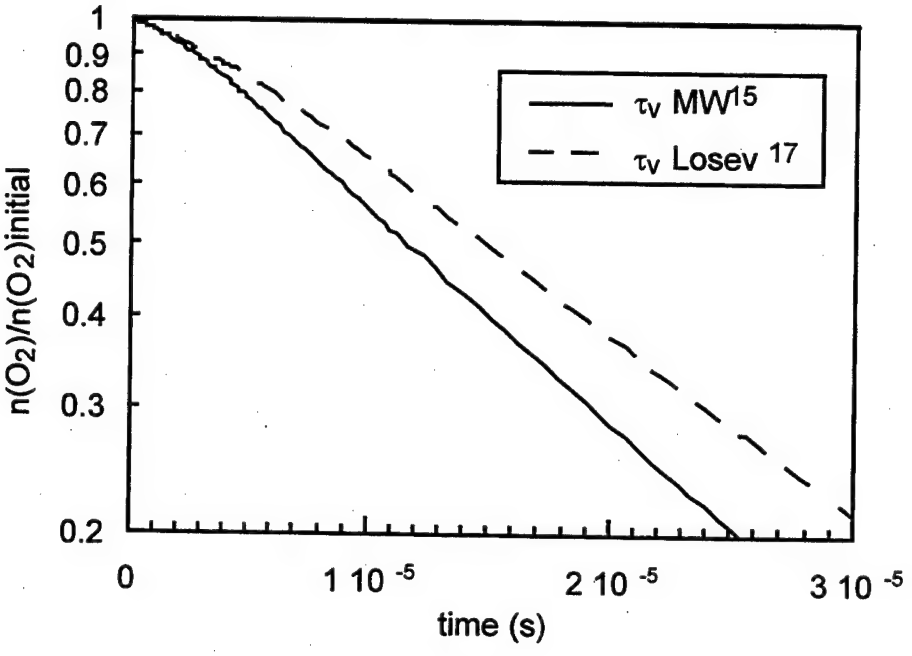

Figure 5(a)
Effect of τ_V on Rate of Nonequilibrium Dissociation

Figure 5(b) shows the effect of vibrational favoring in the dissociation model. The four cases shown all use Model III for VT, but use EAE[28] dissociation or Koura[28] dissociation with $\lambda = 0$, 1, and 2 to vary the amount of vibrational favoring, which results in a change in k_d* of about a factor of 2. Also included in the figure for comparison is an indication of the equilibrium dissociation rate constant predicted by the current models to re-emphasize that k_d* is significantly reduced from k_d^{eq} even with no vibrational favoring (EAE model). Table 1 summarizes the results for k_d* and τ_{inc} for a number of simulations. Also included are experimentally measured values for τ_{inc} and k_d*, but, since dissociation models typically have an adjustable steric factor, only the ratio of k_d^{eq}/k_d* is truly significant, and a measured value of k_d* without a known value of k_d^{eq} cannot be used to distinguish among various models.

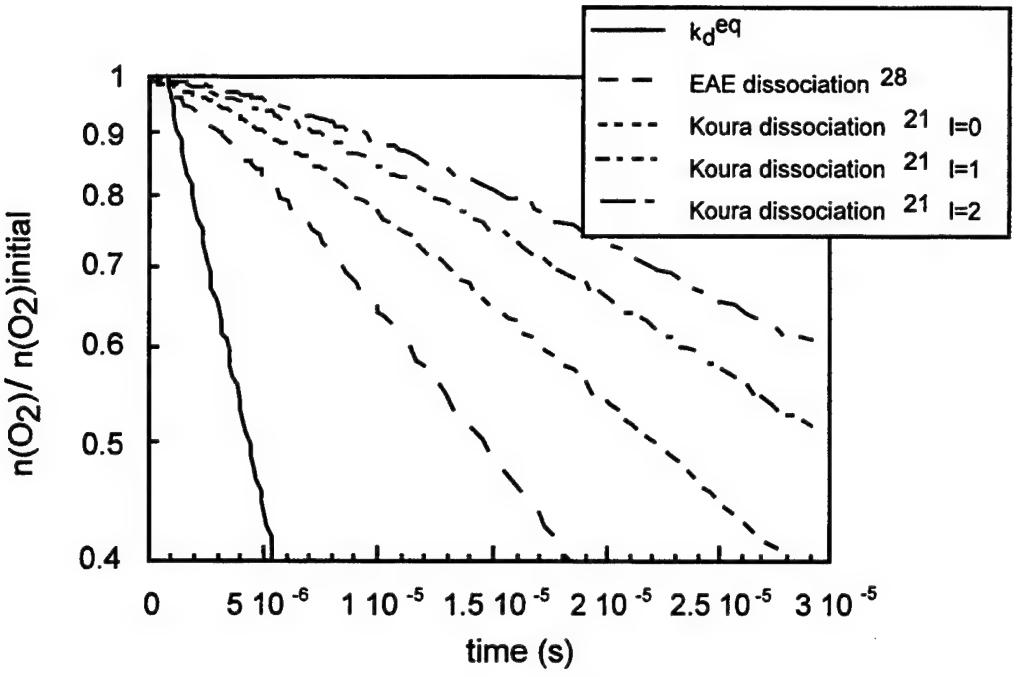

Figure 5(b)
Effect of Varying Amount of Vibrational Favoring on Nonequilibrium Rate of Dissociation
A line showing the rate of equilibrium dissociation is included for comparison

Table 1. Simulation Results for Nonequilibrium Dissociation of O_2 in Argon at 7000 K

	τ_{inc} (μsec)	k_d* (x10^{19} m^3/s)	k_d^{eq}/k_d*
Model II, MW τ_V, EAE dissociation[28]	1.4	5.2	1.5
Model II, Losev τ_V, EAE dissociation[28]	2.2	4.3	1.9
Model III, EAE dissociation[28]	2.1	4.4	1.8
Model III, Koura[21] dissociation, $\lambda = 0$	3.0	2.8	2.8
Model III, Koura[21] dissociation, $\lambda = 1$	3.8	2.0	3.9
Model III, Koura[21] dissociation, $\lambda = 2$	4.5	1.6	5.0
Measured – Wray[26]	4-5	8	N/A

Figure 6 shows the quasi-steady state VDF for the same simulations presented in Figure 5(b). For each vibrational level, $f(v)/f^{eq}(v)$ is plotted – the fraction of O_2 molecules in that level divided by the fraction that would be present in a Boltzmann distribution at 7000 K. Notice that, because $f(v)/f^{eq}(v)$ dips below 1 for the middle and high vibrational levels, it must be greater than 1 for the lowest levels. This behavior is predicted by Haug, *et al.* for the H_2-argon system.[57] This figure may be compared with Figure 7 of Reference 20 which plots the same quantity for the TCE and VFD dissociation models for O_2-argon, also at 7000 K (Reference 20 uses anharmonic oscillator energy levels, but the behavior at the same value of E_V/D should be the same). The TCE result from that plot and the EAE result in Figure 6 here should be the same, except for the following two differences. First, the overall τ_V for the simulations shown in Figure 6 (ITFITS VT model) is significantly greater than the τ_V value (based on Camac's correlation) assumed in

Reference 20. Second, the dissociation models in Reference 15 have been adjusted to agree with Marrone's recommendation for k_d^{eq}, which is a factor of 2.5 lower than k_d^{eq} produced by the EAE model. Both of these differences will tend to drive the quasi-steady state VDFs shown in Figure 6 farther away from a Boltzmann distribution than the cases shown in Reference 20. This provides another example of the sensitivity of nonequilibrium simulation results to the details of the model inputs. The trend that can be seen in Figure 6 is that increasing the amount of vibrational favoring in the dissociation model will drive the quasi-steady state VDF down for the very highest vibrational levels, but up in the intermediate levels.

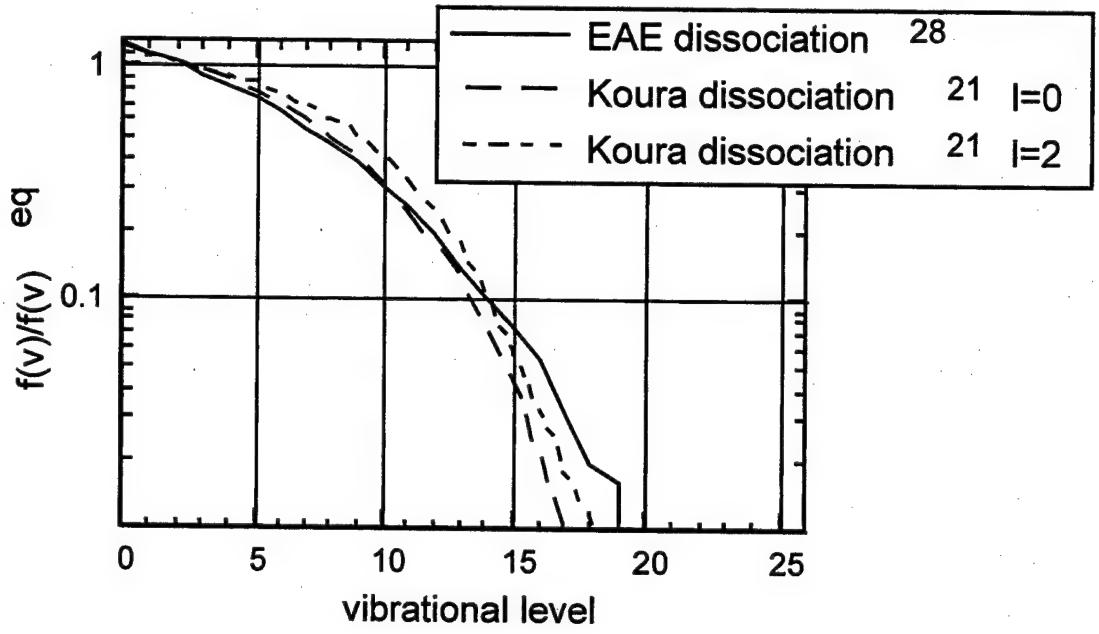

Figure 6
Quasi-steady-state Vibrational Distribution Function with Different Amounts of Vibrational Favoring

CONCLUSIONS

For the atom exchange reactions relevant to air chemistry (Zel'dovich reactions), there exists reasonable validation that a chemistry model based on the total collision energy without vibrational favoring is adequate. For dissociation reactions, a number of studies have used shock tube data of nonequilibrium dissociation rate constants to show that a vibrational favoring effect is very likely. More detailed model validation cannot be obtained from shock data, however, without additional confidence in the estimated value of k_d^{eq} and in the VT model, since the uncertainties in these quantities cause effects of about the same magnitude as the effects of variations in the dissociation model. It seems likely that a fairly simple computational model will be able to capture the important aspects of chemically reacting nonequilibrium flows. However, true validation of the chemistry models used in DSMC will require detailed state-specific measurements or QCT or other type of calculation of rate constants or, better yet, energy-dependent cross sections. Currently available data do not permit an evaluation of which model best simulates nonequilibrium air dissociation reactions. This study emphasizes the need for a

careful evaluation of any proposed verification experiment as to whether it will provide sufficient information to distinguish between different DSMC chemistry models.

REFERENCES

1. Boyd, I.D., G.V. Candler, and D.A. Levin, "Dissociation Modeling in Low Density Hypersonic Flows of Air," *Phys. Fluids,* **7**, *7*, Jul 1995, pp. 1757-63.

2. Treanor, C.T., I.A. Adamovich, M.J. Williams, and J.W. Rich, "Kinetics of NO formation Behind Strong Shock Waves," AIAA 95-2061, presented at the 30th Thermophysics Conference, San Diego, CA, June 19-22, 1995.

3. Levine, R.D., and R.B. Bernstein, **Molecular Reaction Dynamics and Chemical Reactivity**, Oxford Univ. Press, 1987.

4. Levine, R.D., and J. Manz, "The Effect of Reagent Energy on Chemical Reaction Rates: an Information Theoretic Approach," *J. Chem. Phys.*, **63**, *10*, 15 Nov 75, pp. 4280-303.

5. Marriott, P.M., and J.K. Harvey, "A New Approach for Modelling Energy Exchange and Chemical Reactions in the Direct Simulation Monte Carlo Method," **Rarefield Gas Dynamics: Proceedings of the 17th International Symposium on Rarefied Gas Dynamics, July 8-14, 1990, Aachen, Germany**, pp. 784-91.

6. Gallis, M.A., and J.K. Harvey, "Implementation of a Maximum Entropy Method in Monte Carlo Direct Simulations," AIAA 95-2094, presented at the 30th Thermophysics Conference, San Diego, CA, June 19-22, 1995.

7. Black, G., R.L. Sharpless, and T.G. Slanger, "Measurements of Vibrationally Excited Molecules by Raman Scattering. I. The Yield of Vibrationally Excited Nitrogen in the Reaction N+NO to N_2+O," *J. Chem. Phys.* **58**, *11*, 1 Jun 1973, pp. 4792-7.

8. Winkler, I.C., R.A. Stachnik, J.I. Steinfeld, and S.M. Miller, "Determination of NO(v=0-7) Product Distribution from the N^4S+O_2 Reaction Using Two-Photon Ionization," *J. Chem. Phys.*, **85**, *2*, 15 Jul 1986, pp. 890-9.

9. Bose, D., and G.V. Candler, "Thermal Rate Constants of the N_2+O to NO+N reaction Using *ab initio* $^3A''$ and $^3A'$ Potential Energy Surface," *J. Chem. Phys.*, **104**, *8*, 22 Feb 1996, pp. 2825-33.

10. Bose, D., and G.V. Candler, "Kinetics of the N_2+O to NO+N Reaction in Nonequilibrium Flows," AIAA-96-0104, presented at the 34th Aerospace Sciences Meeting and Exhibit, Reno, NV, Jan. 15-18, 1996.

11. Blais, N.C., and D.G. Trular, "Monte Carlo Trajectory Study of Ar+H_2 Collisions. II Vibrational and Rotational Enhancement of Cross Sections for Dissociation," *J. Chem. Phys.*, **66**, *2*, 15 Jan 1977, pp. 772-8.

12. Rebick, C., and R.D. Levine, "Collisions Induced Dissociation: a Statistical Study," *J. Chem. Phys.*, **58**, *9*, 1 May 1973, pp. 3942-52.

13. Dove, J.E., and M.E. Mandy, "A Quasiclassical Trajectory Study of the Collisional Dissociation of H_2 by H Atoms," *Int. J. Chem. Kinetics*, **18**, *9*, 1986, pp. 993-1007.

14. Marrone, P.V., and C.E. Treanor, "Chemical Relaxation with Preferential Dissociation from Excited Vibrational Levels," *Phys. Fluids*, **6**, *9*, Sep 1963, pp. 1215-21.

15. Millikan, R.C., and D.R. White, "Systematics of Vibrational Relaxation," *J. Chem. Phys.*, **39**, *12*, 1963, pp. 3209-3213.

16. Camac, M., "O_2 Vibrational Relaxation in Oxygen-Argon Mixtures," *J. Chem. Phys.*, **34**, *2*, 1961, pp. 448-459.

17. Losev, S.A., and O.P. Shatalov, "The Vibrational Relaxation of Oxygen Molecules in Admixture with Argon at Temperatures up to 10,000 K," *Khimiya Vysokikh Energii*, **4**, *3*, 1970, pp. 263-267.

18. Macheret, S.O., and J.W. Rich, "Nonequilibrium Dissociation Rates Behind Strong Shock Waves: Classical Model," *Chem. Phys.*, **174**, *1*, 15 Jul 1993, pp. 25-43.

19. Kiefer, J.H., and J.C. Hajduk, "A Vibrational Bias Mechanism for Diatomic Dissociation: Induction Times and Steady Rates for O_2, H_2, and D_2 Dilute in Ar," *Chem. Phys.*, **38**, *3*, 1 May 1979, pp. 329-40.

20. Haas, B.L., and I.D. Boyd, "Models for Direct Monte Carlo Simulation of Coupled Vibration-Dissociation," *Phys. Fluids A-Fluid Dynamics*, **5**, *2*, Feb 1993, pp. 478-89.

21. Koura, K., "A Set of Model Cross Sections for the Monte Carlo Simulation of Rarefied Real Gases: Atom-Diatom Collisions," *Phys. Fluids*, **6**, *10*, Oct 1994, pp. 3473-86.

22. Gonzales, D.A., and P.L. Varghese, "A Simple Model for State-Specific Diatomic Dissociation," *J. Phys. Chem.*, **97**, *29*, 22 Jul 1993, pp. 7612-22.

23. Gonzales, D.A., and P.L. Varghese, "Evaluation of Simple Rate Expressions for Vibration-Dissociation Coupling," *J. Thermophys. Heat Trans.*, **8**, *2*, Jun 1994, pp. 236-43.

24. Shizgal, B.D., and F. Lordet, "Vibrational Nonequilibrium in a Supersonic Expansion with Reaction: Application to O_2-O," *J. Chem. Phys.*, **104**, *10*, 8 Mar 1996, pp. 3579-97.

25. Keck, J., and G. Carrier, "Diffusion Theory of Nonequilibrium Dissociation and Recombination," *J. Chem. Phys.*, **43**, *7*, 1965, pp. 2284-98.

26. Wray, K., "Shock Tube Study of the Coupling of the O^2-Ar Rates of Dissociation and Vibrational Relaxation," *J. Chem. Phys.*, **37**, *6*, 1962, pp. 1254-63.

27. Camac, M., and A. Vaughan, "O_2 Dissociation Rates in O_2-Ar Mixtures," *J. Chem. Phys.*, **34**, *2*, 1961, pp.460-70.

28. Bird, G.A., **Molecular Gas Dynamics and the Direct Simulation of Gas Flows**, Oxford Engineering Science Series 42, Clarendon Press, Oxford, 1994.

29. Haas, B.L., D.B. Hash, G.A. Bird, F.E. Lumpkin, and H.A. Hassan, "Rates of Thermal Relaxation in Direct Simulation Monte Carlo Methods," *Phys. Fluids*, **6**, *6*, Jun 1994, pp. 2191-201.

30. Koura, K., and H. Matsumoto, "Variable Soft Sphere Molecular Model for Air Species," *Phys. Fluids A-Fluid Dynamics*, **4**, *5*, May 1992, pp. 1083-5.

31. White, D.R., and R.C. Millikan, "Oxygen Vibrational Relaxation in O_2-Ar Mixtures," *J. Chem. Phys.*, **39**, *7*, 1963, pp. 1807-08.

32. Borgnakke, C., and P.S. Larsen, "Statistical Collision Model for Monte Carlo Simulation of Polyatomic Gas Mixture," *J. Comput. Phys.*, **18**, 1 Aug 1975, pp. 405-20.

33. Boyd, I.D., "Analysis of Vibrational-Translational Energy-Transfer Using the Direct Simulation Monte-Carlo Method," *Phys. Fluids A-Fluid Dynamics*, **3**, *7*, 1991, 1785-91.

34. Abe, T, "Inelastic-Collision Model for Vibrational-Translational and Vibrational-Vibrational Energy-Transfer in the Direct Simulation Monte Carlo Method," *Phys. Fluids,* **6**, *9*, Sep 1994, pp. 3175-79.

35. Choquet, I., "Vibrational Nonequilibrium Modeling Using Direct Simulation. Part I: Continuous Internal Energy," *J. Thermophys. Heat Transfer*, **9**, *3*, Jul-Sep 1995, pp. 446-55.

36. Koura, K., "Molecular Model for Monte Carlo Simulation of Rarefied Real Gases," **Rarefied Gas Dynamics: Proceedings of the 19th International Symposium Held at the University of Oxford, 25-29 July 1994 (International Symposia)**, J. Harvey and G. Lord, eds., Oxford Univ. Press, 1995, pp. 483.

37. Heidrich, F.E., K.R. Wilson, and D. Rapp, "Collinear Collisions of an Atom and Harmonic Oscillator," *J. Chem. Phys.*, **54**, *9*, 1 May 1971, pp. 3885-97.

38. Kerner, E.H., "Note on the Forced and Damped Oscillations in Quantum Mechanics," *Canadian J. Phys.*, **36**, 1958, pp. 371.

39. Treanor, C.E., "Vibrational Energy Transfer in High-Energy Collisions," *J. Chem. Phys.*, **43**, 2, 1965, pp. 532-38.

40. Adamovich, I.V., S.O. Macheret, J.W. Rich, and C.E. Treanor, "Vibrational Relaxation and Dissociation Behind Shock Waves. Part 1: Kinetic Rate Models," and "Part 2: Master Equation Modeling," *AIAA J.*, **33**, *6*, Jun 1995, pp. 1064-1075.

41. Billing, G.D., and R.E. Kolesnick, "Vibrational Relaxation of Oxygen. State to State Rate Constants," *Chem. Phys. Lett.*, **200**, *4*, 11 Dec 1992, pp. 382-6.

42. Billing, G.D., and E.R. Fischer, "VV and VT rate Coefficients in N_2 by a Quantum-Classical Model," *Chem. Phys.*, **43**, 1979, pp. 395.

43. Bird, G.A., "Simulation of Multi-Dimensional and Chemically Reacting Flows," **Rarefied Gas Dynamics: Proceedings of the 11th International Symposium, Cannes, France, July 3-8, 1978**, R. Campargue, ed., 1 Jan 79, pp. 365-88.

44. Bird, G.A., "New Chemical Reaction Model for Direct Simulation Monte Carlo Studies," **Rarefied Gas Dynamics – Theory and Simulations: Proceedings of the 18th International Symposium on Rarefied Gas Dynamics,** University of British Columbia, Vancouver, Canada, Jul 26-30, 1992, B.D. Shizgal and D.P. Weaver, eds., pp. 185-96 (Available from AIAA, Washington, D.C., 1994).

45. Carlson, A.B., and G.A. Bird, "Implementation of a Vibrationally Linked Chemical Reaction Model," **Rarefied Gas Dynamics: Proceedings of the 19th International Symposium Held at the University of Oxford, 25-29 July 1994 (International Symposia)**, J. Harvey and G. Lord, eds., Oxford Univ. Press, 1995.

46. Wadsworth, D.C.. and I.J. Wysong, "Examination of DSMC Chemistry Models: Role of Vibrational Chemistry Model," **Rarefied Gas Dynamics 20**, C. Shen, ed., Peking Univ. Press, Beijing, 1997, pp. 174-179.

47. Hash, D.B., and H.A. Hassan, "Direct Simulation with Vibration-Dissociation Coupling," *J. Thermophys. Heat Transfer*, 7, *4*, Oct-Dec 1993, pp. 680-6.

48. Gimelshein, S.F., M.S. Ivanov, G.N. Markelov, and Yu E. Gorbachev, "Quasiclassical VRT Transition Models in the DSMC Computations of Reacting Rarefied Flows," **Rarefied Gas Dynamics 20**, C. Shen, ed., Peking Univ. Press, Beijing, 1997, pp. 711-716.

49. Warnatz, J., U. Reidel, and R. Schmidt, "Different Levels of Air Dissociation Chemistry and Its Coupling with Flow Models," **Advances in Hypersonics, Vol. 2 – Modeling Hypersonic Flows**, 1 Jan 1992, pp. 67-103.

50. Boyd, I.D., "A Threshold Line Model for the Direct Simulation Monte Carlo Method," *Phys. Fluids*, **8,** *5*, May 1996, pp. 1293-1300.

51. Gupta, R.N., J.M. Yos, R.A. Thompson, and K-P Lee, "A Review of Reaction Rates and Thermodynamic and Transport Properties for an 11-Species Air Model for Chemical and Thermal Nonequilibrium Calculations to 30000 K," NASA RP-1232, NASA Langley Research Center, 1 Aug 1990.

52. Baulch, D.L., D.D. Drysdale, J. Duxbury, and S.J. Grant, **Evaluated Kinetic Data for High Temperature Reactions, Vol. 3**, Butterworth's, London, 1976.

53. Kafri, A., "Computations and Applications of Classical Phase Space Integrals in Reactive Molecular Collisions," *Chem. Phys.*, **13**, *4*, 15 Apr 1976, pp. 309-21.

54. Kafri, A., and R.D. Levine, "Comment on the Dynamics of Dissociation of Diatomic Molecules: Mass and Temperature Effects," *J. Chem. Phys.*, **64**, *12*, 15 Jun 1976, pp. 5320-21.

55. Kondriatev, V.N. and E.E. Nikitin, "Rate Constants for the Process O_2+Ar to O+O+Ar," *J. Chem. Phys.*, **45**, 1966, pp. 1078-9.

56. Jerig, L., K. Thielen, and P. Roth, "High Temperature Dissociation of Oxygen Diuluted in Argon or Nitrogen," *AIAA J.*, **29**, *7*, 1991, pp. 1136-39.

57. Haug K., D.G. Trular and N.C. Blais, "Monte Carlo Trajectory and Master Equation Simulation of the Nonequilibrium Dissociation Rate Coefficient for Ar+H_2 to Ar+2H at 4500 K," *J. Chem. Phys.*, **86**, *5*, 1 Mar 1987, pp. 2697-716.

PART II: EXAMINATION OF DSMC CHEMISTRY MODELS: ROLE OF VIBRATIONAL FAVORING

INTRODUCTION

An accurate model of chemical reactions is a key factor in obtaining useful predictions of radiation and surface heating around re-entry vehicles or spacecraft and in understanding plasma processing environments, etc. These types of flows, however, typically display significant thermal and chemical nonequilibrium. The degree of population of high vibrational levels is often the controlling factor in the probability of dissociation and endoergic exchange reactions.

Direct Simulation Monte Carlo (DSMC) calculations, which simulate individual gas particle collisions, are well suited to the inclusion of physically accurate chemistry models based on the translational and internal energy states of each molecule. A minimum requirement for a DSMC chemistry model would be to reasonably reproduce known equilibrium rate constants. A second requirement is to reasonably reflect the relative probabilities for reaction for molecules in different internal energy states, thus allowing realistic modeling of gases where the distribution of internal energies is far from equilibrium. A number of proposed chemistry models have been demonstrated to meet the first requirement. The present study concentrates on questions relating to the second requirement.

Some chemical reactions are known to have their reaction probability enhanced by vibrational excitation of the reactants. This characteristic will be referred to as "vibrational favoring." Any endoergic reaction will be enhanced by vibrational excitation, merely because the amount of total energy available in the collision is increased (assuming that all types of energy contribute to the activation energy). "Vibrational favoring" refers to an increase in reaction probability beyond what would be expected due to the amount of total energy available and indicates that vibrational energy is more effective than other types of energy in promoting reaction.

EXACT AVAILABLE ENERGY (EAE) MODEL

The method introduced by Bird[1] to simulate chemical reactions in DSMC calculations, sometimes referred to as total collision energy (TCE) model, is widely utilized. It uses adjustable parameters to reproduce measured reaction rate coefficients as a function of temperature under equilibrium conditions. The number of energy modes of the reacting molecules contributing to the reaction probability is an input parameter in the TCE model. It can range from the sum of all internal energy and translational energy to only including translational energy modes.

Bird and Carlson have introduced a different DSMC method for chemical reactions,[2,3] known as the exact available energy (EAE) approach (it has also been referred to as a vibrationally linked chemistry approach). It does away with reaction rate constants as such and allows dissociation or atom exchange whenever the post-collision vibrational energy based on Borgnakke-Larsen (BL) redistribution reaches or exceeds the activation energy. Under equilibrium conditions, this method has been shown[2,3] to reproduce the correct order of magnitude for the dissociation rates of O_2-O_2 and N_2-N_2 as well as the Zel'dovich air exchange reaction rates as a function of temperature. Like the TCE method, the EAE is based on the total energy of a collision, with no favoring of vibrational energy.

Other models generally use input parameters that are adjusted to reproduce "known" equilibrium rate constants that are in fact not well known at high temperatures. Thus, one interesting feature of the EAE model is that it does not use adjustable input parameters.

However, there is some variability in results for dissociation due to the use of "notional" vibrational levels. These are assumed vibrational levels that extend above the dissociation energy (D) with a suggested spacing either equal to,[2] or one-half of,[3] the spacing of the two highest bound vibrational levels. The BL vibrational redistribution method chooses a post-collision level based on the total pre-collision energy. If the post-collision level is above D, then a dissociation reaction is assumed to have taken place. In this study, it has been found that the choice of the energy spacing of the notional levels has a direct effect on the equilibrium dissociation rate constant that is predicted by the EAE model, with the rate constant decreasing as the spacing of the notional levels increases.

It should be noted that the probabilities for recombination and reverse exchange reactions for the EAE chemistry model are given in Reference 2 based on equilibrium collision theory and calculated partition functions. But, since the forward dissociation probability depends on the notional level spacing, the expression for the recombination probability must be adjusted depending on the spacing used for the notional levels in order to correctly reproduce the equilibrium fraction of dissociation. Also, as pointed out in Reference 2, the EAE model for dissociation is nearly independent of collision partner (except for small changes due to reduced mass and variable hard sphere (VHS) collision parameter ω), and so does not allow for the so-called third body probability term. Since the measured dependence on collision partners typically has a large experimental uncertainty, however, it is difficult to assess the impact of this feature of the model.

ATOM EXCHANGE REACTIONS

For air chemistry, the two Zel'dovich exchange reactions are important, one of which is:

$$N2(v) + O \leftrightarrow NO + N \qquad (1)$$

It is known[4-6] that some endoergic atom exchange reactions display a large vibrational favoring effect, while others display virtually no preference for vibrational energy as compared to other types of energy. It has been argued previously[6-8] that information from the vibrational energy distribution in the products of the reverse (exoergic) reaction, along with detailed balance arguments, can be used to determine whether an endoergic exchange reaction is strongly vibrationally favored or not. Based on this approach, it was predicted that the Zel'dovich reactions will not have significant vibrational favoring. For a reaction where vibrational favoring is not significant, a chemistry model that is based on the total collision energy (such as the EAE model) will be adequate.

Recent quasi-classical trajectory (QCT) calculations[9,10] of state-to-state reaction cross sections provide valuable detailed information for Reaction (1). In light of this new information, Boyd *et al.* have proposed[9] a generalized collision energy (GCE) model that modifies the TCE model with three adjustable terms to separately weight the amount of translational, rotational, and vibrational energy of the reactants. One measure of the performance of the GCE model is given by comparing the distribution of the nitrogen molecules that are selected for reaction by the DSMC code with the distribution predicted by the QCT results for two different temperature conditions. (This distribution is proportional to the product of the relative reaction rate constant for each vibrational level and the relative population of that level). Excellent agreement is seen.

In order to test the assertion that a chemistry model based on the total collision energy (such as the EAE model) will be adequate for this reaction, the same two temperature conditions for Reaction (1) were simulated using a DSMC code with the EAE chemistry model. The results are shown in Figure 1 for the equilibrium case with T = 5000 K and in Figure 2 for the nonequilibrium case with translational temperature, T_{rans} = 14,000 K, rotational temperature, T_{rot}

= 5000 K, and vibrational temperature, T_{vib} = 1000 K. The QCT results are also shown in the figures. As expected, the agreement is quite good. Thus, the increased production of NO in the bow shock case that has been observed with the implementation of the GCE model[10] is likely due to the larger overall rate constant for Reaction (1) rather than the dependence on internal energy state distribution.

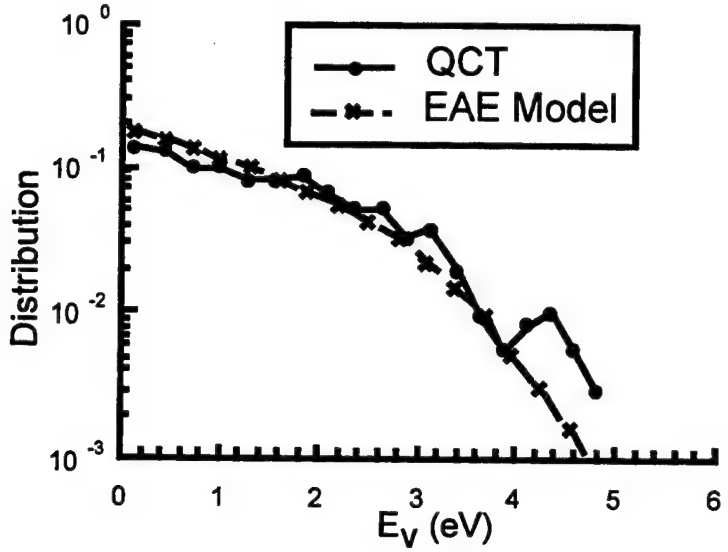

Figure 1
Vibrational Distribution of Reacting N_2 Molecules. $T_{trans} = T_{rot} = 5000$ K

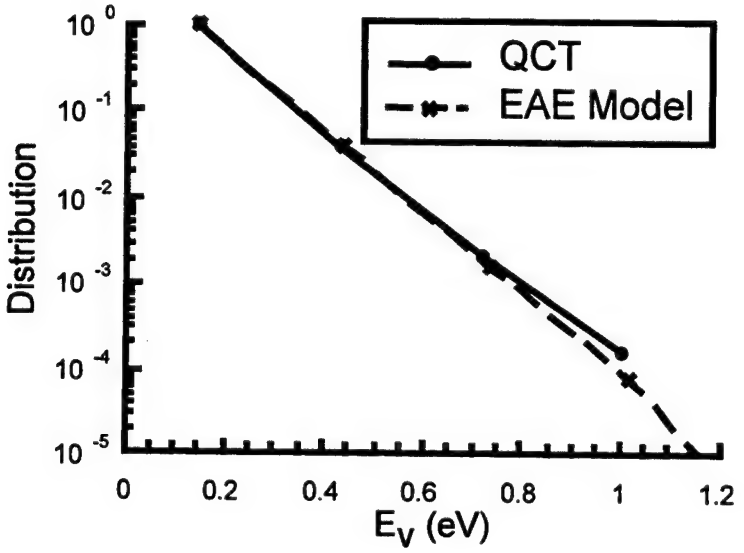

Figure 2
Vibrational Distribution of Reacting N_2 Molecules.
T_{trans} = 14000 K, T_{rot} = 5000 K, T_{vib} = 1000 K

DSMC DISSOCIATION MODELS

Collision-induced dissociation reactions of diatomic molecules are often considered to be vibrationally favored, yet unambiguous information on the degree of favoring is scant. The number of methods that have been used in the context of DSMC simulations is fairly limited. In addition to the TCE and EAE models described above, Haas and Boyd[11,12] introduced the vibrationally favored dissociation (VFD) model which modifies the TCE model and allows for favoring of vibrational energy (E_V) in the dissociation probability through an adjustable (empirical) exponent parameter, ϕ. Ivanov, *et al.** have implemented a dissociation model in their DSMC code that uses probabilities based on state-specific rate constants that include a certain (fixed) amount of vibrational favoring.

Macheret and Rich[11,12] have presented an analytical threshold line model which includes E_{tr}, E_r, and E_V as parameters. Recently, Boyd[13] has adapted this model for a DSMC implementation, using one probability expression for dissociation from high vibrational levels and a different (reduced) probability expression for low vibrational levels. The reduction in probability for lower levels means that this model is vibrationally favored. For the case of N_2-N_2 presented in Reference 13, the transition occurs around v = 6. This model has one adjustable parameter that is used to match the equilibrium dissociation rate constant at some temperature, but uses no adjustable parameter relating to the degree of vibrational favoring. Boyd has shown that the prediction of the threshold line model for the equilibrium dissociation rate constant as a function of temperature is reasonable. The threshold line model as described in Reference 13 has been implemented in the code, but the effect of mathematical singularities[11,12] near certain values of vibrational energy has been observed to be significant. Use of the full threshold model[11,12] rather than the simplified model[13] reduces the effect of the singularities and limits the spurious peak that occurred in the region of the transition vibrational level as can be seen in Figure 3 for the case of H_2 dissociation. Details of the implementation are given in Reference 14. The H_2 threshold line model results shown in Figures 4 and 5 here all used the corrected version of the model.

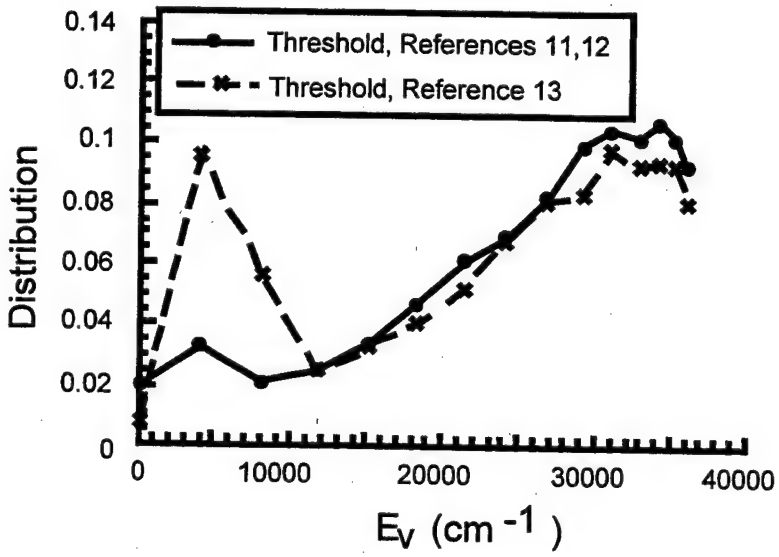

Figure 3
Threshold Dissociation Model Results for H_2 + H; Effect of Singularities

*Ivanov, M.S., Gimelshein, S.F., Kashovsky, A.V., and Markelov, G.N., private communication.

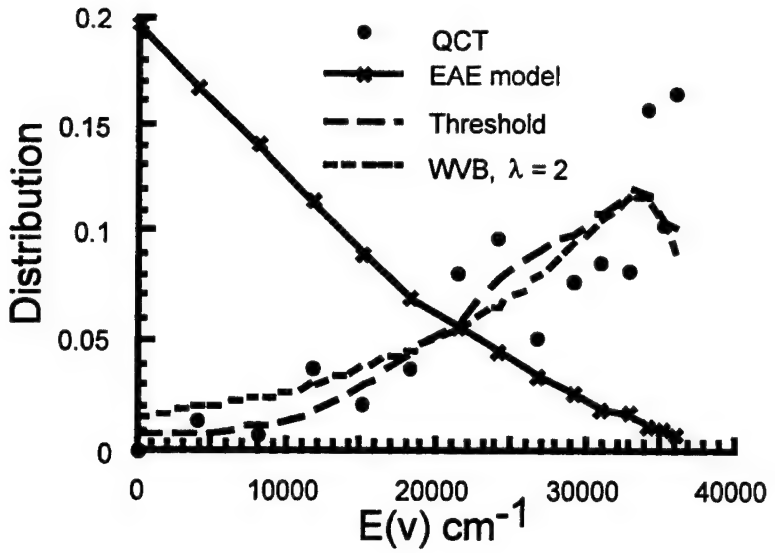

Figure 4
Comparison of QCT Results for H_2 + Ar with DSMC Dissociation Models

Figure 5

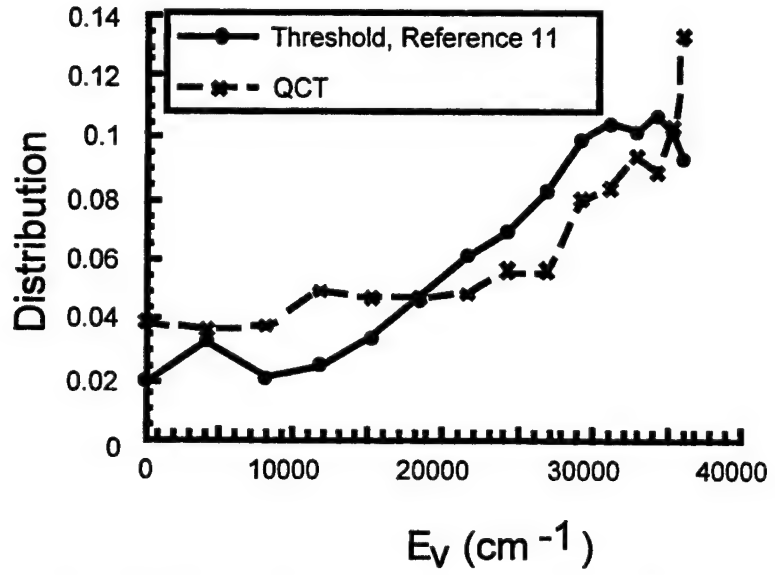

Threshold Dissociation Model for H_2 + H; Comparison with QCT Results

The works of Levine, *et al.*[4,5] describe in detail a compact method to quantify the enhancement of chemical reactions due to reactant internal energy using a single parameter, λ. When $\lambda = 0$, then there is no vibrational favoring, and the reaction probability is increased by all types of energy equally. The magnitude of λ indicates the degree of vibrational favoring. An approach to modeling vibrationally favored dissociation based on the formalism of Levine has been used in several studies[15-18] for continuum simulations of nonequilibrium gases. For particle simulations, Marriott,[19] Gallis,[20] and Koura[21] have presented adaptations of the Levine approach; all of these include an adjustable parameter, λ, that indicates the degree of vibrational

favoring, but formulated in different ways. Koura bases his dissociation model on the weak vibrational bias (WVB) equation of Reference 20 and recommends $\lambda = 2$ for O_2-argon.

The method of displaying the vibrational distribution of the reacting molecules shown in Figure 3 (and in Figures 1 and 2 for the case of an exchange reaction) is useful in visualizing the differences in dissociation models. This has been used by Boyd,[13] who compares the probability distribution for N_2-N_2 dissociation in equilibrium at 10,000 K for the VFD (using an estimated value of ϕ) and threshold line models. The results demonstrate that, even though two models may reproduce the same equilibrium dissociation rate constant and both are vibrationally favored, they may have very different behaviors at the state-specific level. Unfortunately, state-specific information is not available for N_2 dissociation (or for O_2), so choosing the most realistic model is difficult. A previous study[6] addressed some of the difficulties in using shock tube data to distinguish between chemistry models with different amounts of vibrational favoring. Shock tube measurements are typically of macroscopic parameters (such as a nonequilibrium dissociation rate constant and dissociation induction time), which are not very sensitive to the probability distribution and do not provide the state-specific information desired to validate a DSMC model.

To begin to address these issues, this study made use of the state-specific dissociation results that are available from QCT calculations for H_2. Truhlar, *et al.*[22] have obtained vibrational state (rotationally averaged) dissociation rate constants for H_2 dissociation in collisions with argon at 4500 K. Also, Martin and Mandy[23] obtained dissociation rate constants for every vibration-rotation level of H_2 colliding with H for the entire temperature range of 450-45,000 K. In order to obtain rotationally averaged results for the H_2-H case, the rate constants for each rotational level within a given vibrational level have been appropriately weighted (according to degeneracy and Boltzmann fraction) and summed over.

For the first comparison, an equilibrium case for H_2-argon at 4500 K was calculated using three DSMC dissociation models: EAE, WVB as described in Reference 20, and threshold line model. Figure 4 compares the QCT results[22] with DSMC calculations for the EAE, threshold, and WVB models' predictions of the vibrational distribution of dissociating H_2. The WVB model result is shown for $\lambda = 2$. The model was also run for $\lambda = 4$, which is not shown. Increasing λ causes the distribution to be peaked more toward higher v and the two values bracket the QCT points quite well. (Reference 22 states that a fit of their results to the WVB equation yields a value of $\lambda = 2.2$, but the fit in this study using Truhlar's result yields $\lambda = 2.8$). The probability distribution shape of the EAE, with no vibrational favoring, is significantly different than the QCT result. The WVB model reproduces the correct shape when one uses the proper value of λ, but there is the problem of how one is to obtain λ for any molecule. The threshold line model, with no adjustable parameter, shows very favorable agreement with the QCT result.

Very similar results are shown for H_2-H dissociation in Figure 5 for the threshold model compared with QCT results[23] at 4500 K. The EAE and WVB results for this case are not shown, but give basically the same shape for H_2-H as for H_2-Ar. The QCT results for H_2-H provide some information on how the probability distribution should change with temperature. The state-specific QCT results[21] have been converted to thermal rotationally averaged values for three temperatures: 1000 K, 4500 K, and 20,000 K. The vibrational probability distributions for the three temperatures are compared in Figure 6. As can be seen, the effect of vibrational favoring becomes less pronounced as the temperature increases. This trend is predicted in the works of Levine[4,5] who formulate an expression for vibrational favoring as $\exp(-\lambda * E_V/kT)$. This expression has been shown to be realistic for exchange reactions where a translation-rotation temperature exists, but is not suited to DSMC calculations. The WVB model does not include any provision for a reduction in vibrational favoring at higher temperatures, and so may be expected to be realistic over some range of temperatures, but less so as the range becomes very wide. Preliminary results using the threshold line model indicate this model may produce a reduction in vibrational favoring as temperature is increased, but further studies are needed.

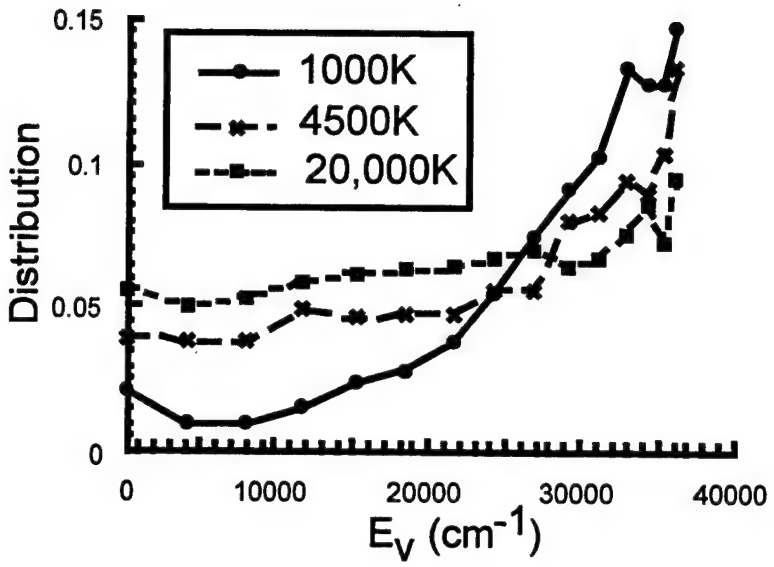

Figure 6
QCT Results for Temperature Dependence of Vibrational Favoring in H_2 + H Dissociation

CONCLUSIONS

Comparisons with QCT results for the first Zel'dovich reaction confirm that the EAE chemistry model gives a very realistic dependence on internal energy states for a reaction that is not vibrationally favored. Naturally, it is not to be expected that the probability distribution predicted by the EAE model will be accurate in the case of an exchange reaction that is known to be strongly vibrationally favored,[4,5] such as HCl + I.

For the case of H_2 dissociation, the WVB model with $\lambda = 2$ to 4 and the threshold line model give qualitative agreement with QCT results, showing the correct type of vibrational favoring effect. It should be noted, however, that the H_2 molecule is not necessarily representative of other diatomics. Its widely spaced rotational and vibrational levels cause quantum effects to play a more important role. Accurate state-specific dissociation probabilities or rate constants are needed for other diatomic molecules to further assess DSMC models.

REFERENCES

1. Bird, G.A., "Simulation of Multi-Dimensional and Chemically Reacting Flows," **Rarefied Gas Dynamics: Proceedings of the 11th International Symposium, Cannes, Frances, July 3-8, 1978**, R. Campargue, ed., 1 Jan 1979, pp. 365-388.

2. Bird, G.A., **Molecular Gas Dynamics and the Direct Simulation of Gas Flows**, Oxford: Engineering Science Series 42, Clarendon Press, Oxford, 1994, pp. 434-440.

3. Carlson, A.B., and Bird, G.A., "Implementation of a Vibrationally Linked Chemical Reaction Model," **Rarefied Gas Dynamics: Proceedings of the 19th International Symposium Held at the University of Oxford, 25-29 July 1994 (International Symposia)**, J. Harvey and G. Lord, eds., Oxford University Press, 1995.

4. Levine, R.D., and Bernstein, R.B., **Molecular Reaction Dynamics and Chemical Reactivity**, Oxford Univ. Press, 1987.

5. Levine, R.D., and Manz, J, "The Effect of Reagent Energy on Chemical Reaction Rates: an Information Theoretic Approach," *J Chem Phys*, **63**, *10*, 15 Nov 75, pp. 4280-303.

6. Wysong, I.J., Wadsworth, D.C., Weaver, D.P., and Campbell, D.H., "Influence of Vibrational Nonequilibrium on Chemically Reacting Rarefied Flows: Toward Experimental Verification of DSMC Models," AIAA 96-2023, presented at the 27th Fluid Dynamics Conference, New Orleans, LA, Jun 17-20, 1996.

7. Bose, D., and Candler, G.V., "Thermal Rate Constants of the N_2+O to NO+N Reaction Using *ab initio* ^{3}A" and ^{3}A' Potential Energy Surface," *J Chem Phys*, **104**, *8*, 22 Feb 96, pp. 2825-33.

8. Bose, D., and Candler, G.V., "Kinetics of the N_2+O to NO+N Reaction in Nonequilibrium Flows," AIAA-96-0104, presented at the 34th Aerospace Sciences Meeting and Exhibit, Reno, NV, Jan 15-18, 1996.

9. Boyd, I.D., Bose, D., and Candler, G.V., "Monte Carlo Modeling of Nitric Oxide Formation Based on Quasi-Classical Trajectory Calculations," AIAA 96-1845, presented at the 31st AIAA Thermophysics Conference, New Orleans, LA, Jun 17-20, 1996.

10. Haas, B.L., and Boyd, ID., "Models for Direct Monte Carlo Simulation of Coupled Vibration-Dissociation, *Phys Fluids A-Fluid Dynamics,* **5**, *2*, Feb 1993, pp. 478-89.

11. Macheret, S.O., and Rich, J.W., "Nonequilibrium Dissociation Rates Behind Strong Shock Waves: Classical Model," *Chem Phys,* **174**, *1*, 15 Jul 1993, pp. 25-43.

12. Macheret, S.O., Fridman, A.A., Adamovich, I.V., Rich, J.W., and Treanor, C.E., "Mechanisms of Nonequilibrium Dissociation of Diatomic Molecules," AIAA 94-1984, presented at the 6th AIAA/ASME Joint Thermophysics and Heat Transfer Conference, Colorado Springs, CO, Jun 20-23, 1994.

13. Boyd, I.D., "A Threshold Line Model for the Direct Simulation Monte Carlo Method," *Phys Fluids*, **8**, *5*, May 1996, pp. 1293-1300.

14. Wadsworth, D.C., and Wsyong, I.J., "Vibrational Favoring Effect in DSMC Dissociation Models," *Phys Fluids*, **9**, *12*, 1997, pp. 3873-3884.

15. Kiefer, J.H., and Hajduk, J.C., "A Vibrational Bias Mechanism for Diatomic Dissociation: Induction Times and Steady Rates for O_2, H_2, and D_2 Dilute in Ar," *Chem Phys,* **38**, *3*, 1 May 1979, pp. 329-340.

16. Gonzales, D.A., and Varghese, P.L., "A Simple Model for State-Specific Diatomic Dissociation," *J Phys Chem*, 97, *29*, 22 Jul 1993, pp. 7612-22.

17. Gonzales, D.A., and Varghese, P.L., "Evaluation of Simple Rate Expressions for Vibration-Dissociation Coupling," *J Thermophys Heat Trans*, 8, *2*, Jun 1994, pp. 236-43.

18. Shizgal, B.D., and Lourdet, F., "Vibrational Nonequilibrium in a Supersonic Expansion with Reaction: Application to O_2-O," *J Chem Phys*, 104, *10*, 8 Mar 1996, pp. 3579-97.

19. Marriott, P.M., and Harvey, J.K., "A New Approach for Modelling Energy Exchange and Chemical Reactions in the Direct Simulation Monte Carlo Method," **Proceedings of the Symposium on Rarefied Gas Dynamics, Aachen, Germany, July 8-14, 1990**, pp. 784-91.

20. Gallis, M.A., and Harvey, J.K., "Implementation of a Maximum Entropy Method in Monte Carlo Direct Simulations," AIAA 95-2094, presented at the 30th Thermophysics Conference, San Diego, CA, Jun 19-22, 1995.

21. Koura, K., "A Set of Model Cross Sections for the Monte Carlo Simulation of Rarefied Real Gases: Atom-Diatom Collisions," *Phys Fluids*, 6, *10*, Oct 1994, pp. 3473-86.

22. Truhlar, D.G., Blais, N.C., Hajduk, J-C.J., and Kiefer, J.H., "Monte Carlo Trajectory Study of Ar+H_2 Collisions: Master-Equation Simulation of a 4500 K Shock Wave Experiment with Thermal Rotation," *Chem Phys Lett*, 63, *2*, 15 May 1979, pp. 337-43.

23. Martin, P.G., and Mandy, M.E., "Analytical Temperature Dependences for a Complete Set of Rate Coefficients for Collisional Excitation and Dissociation of H_2 Molecules by H Atoms," *Astrophys J*, 455, *1/pt. 2*, 10 Dec 95, pp. L89-L92.

PART III: DSMC COMPARISONS TO ROTATIONAL TEMPERATURE MEASUREMENTS IN JET EXPANSIONS WITH FINITE BACKGROUND PRESSURES

INTRODUCTION

A comparison has been made between Direct Simulation Monte Carlo (DSMC) calculations and experimental measurements of rotational temperature in a nitrogen jet expanding into a finite background pressure in which a distinct, but non-continuum, Mach disk is formed.[1] In the work presented in this report, corrections and improvements to various parts of the simulation have been made, a new stagnation region/orifice calculation has been carried out to supply a new startline to the expansion flow calculation, and an investigation of the effects of a revised rotational collision model at low temperatures has been accomplished.

The experimental results that are used for comparison to the simulations were obtained at the University of California at Berkeley Rarefied Gas Wind Tunnel. In those experiments, electron beam fluorescence from the (0,0) vibrational band of the first negative system of the nitrogen ion was used to spectroscopically probe the centerline of a heated nitrogen jet expanding into a chamber maintained at a low but finite background pressure. Centerline rotational temperatures were determined for a number of conditions. A complete description of the experimental procedures and results is presented by Gochberg[2] and a summary is given in Reference 1.

ROTATIONAL RELAXATION MODELS

The prediction of the rotational temperature of a gas in an expansion flow or compression shock, in which large deviations from equilibrium with the translational mode of the gas can occur, is particularly sensitive to the treatment of collisional energy exchange in the simulation. In Reference 1, it was demonstrated that a temperature dependent rotational collision number model produced significantly different rotational temperature profiles in a jet expansion than that of a constant collision number model. In addition, the viscosity coefficient used in the variable hard sphere collision model was also shown to affect the calculated rotational temperatures. Gochberg and Haas[3,4] have examined the effects of rotational relaxation rate models on the rotational temperature in vacuum free jets using an analytical method that involved numerical integration of the governing rotational relaxation rate equations. In comparing the theoretical results to experimental measurements, they were unable to recommend an optimum rotational relaxation model, or combination of models, that would give a good match to all of the experimental data, due primarily to the large degree of scatter in the data. They did conclude that the Parker model[5] does not accurately predict the rotational temperature at low translational temperatures, due to the fact that this model predicts rotational collision relaxation times that go to zero with decreasing temperatures. Quantum effects are known to become significant in rotational relaxation at low temperatures, and the model of Lebed' and Riabov[6] is one example of a method of accounting for these effects. For temperatures below approximately 125 K, quantum effects increase the rotational relaxation time by an order of magnitude or more compared to the Parker model, slowing the equilibration of the rotational mode to the translational mode of the gas.

DSMC SIMULATION

The key features that must be addressed in a DSMC simulation of this problem are the plenum, jet, and vacuum chamber boundary conditions, and the rotational energy relaxation

model.

For the relatively high plenum pressures of the Gochberg experiments it is not possible to do a complete DSMC calculation for the entire plenum-jet system. Therefore, in this study, the calculations were broken up by starting the expansion jet DSMC simulation from a position just upstream of the orifice exit plane. Providing an inflow startline at this position is problematic. The orifice used in the experiments had an l/d of approximately 0.6, and so was not an ideal sonic orifice with Mach 1 at the exit plane. Analysis of these types of tube flows have shown that, along the centerline of the flow, sonic conditions will occur slightly upstream of the exit plane.[7,8] An isentropic expansion from the measured experimental stagnation conditions to sonic conditions (Mach 1) at a position 0.1 mm (0.12 diameters) upsteam of the exit plane was used. A "plug" flow (no boundary layer) was assumed at this position to define the inflow startline for the jet expansion flow calculation. Simulations to determine the effects on centerline jet properties of a full boundary layer were carried out, and the results indicated a finite but small influence of the boundary layer structure as long as the centerline inflow startline parameters were identical.

It would be advantageous to use a full calculation of the flow to better define the conditions at the inflow startline position. DSMC simulation of the flow into the orifice from the stagnation region at the relative high pressures of the experiment (250-550 torr) is difficult even on the largest computers. Navier-Stokes calculations are also difficult due to the fast expansion characteristics of this flow, as well as the difficulty of defining the boundary conditions. The stagnation region DSMC calculation used in Reference 1 had extremely large cells compared to the local mean free path of the gas, and so was unreliable. The pressure-matching method of Serikov[9] was implemented and used for the inflow boundary in the stagnation region. This allowed a calculation to be made using a computational region only 1 orifice diameter upstream of the entrance to the orifice. A calculation of the flow from the stagnation region, through the orifice, and out a small distance into the jet expansion was accomplished on a large parallel computer, allowing cell sizes to be comparable to the local mean free path. This calculation produced sonic conditions well upstream of the exit plane and a much higher translational temperature and velocity than the isentropic expansion prediction. This might be due to the effects of the hot wall on the flow (all walls in the calculation are set to the stagnation region temperature of 753 K). Table 1 presents the centerline values of the flow parameters for the sonic and DSMC startlines at a position 0.1 mm upstream of the orifice exit plane.

Table 1. Inflow Startline Flow Parameters on Centerline

Type	Mach Number	Number Density (m^{-3})	Temperature (K)	Velocity (m/s)
DSMC	1.15	2.49×10^{24}	595	580
Sonic	1.0	2.858×10^{24}	477	445

As in Reference 1, collision energy-dependent rotational collision numbers based on the Parker model,[5] as generalized for variable hard sphere (VHS) molecules by Boyd,[10] was used (with Chung's correction factor[11]), as well as the appropriate low temperature value of w. The corresponding DSMC probabilities of relaxation were based on the methods of Haas, *et al.*[12] This method produces N_2 - N_2 collisional rotational relaxation rates in the DSMC simulation about a factor of 2 higher than the P = 1/Z assumption.

An error in the treatment of the chamber background gas boundary condition in the DSMC calculations was corrected, which eliminated the large difference in the position of the rotational temperature shock between the DSMC prediction and the experimental data that was reported in

Reference 1. Also, various coding errors in the handling of internal energy transfer in collisions were corrected. This prevented a steady loss of rotational energy that was previously occurring.

RESULTS

All of the calculations presented here are for the conditions of Case 1 in Gochberg's[2] experiments: 0.8125 mm diameter orifice, T_o = 753 K, P_o = 351.6 torr, T_∞ = 297.8 K, P_∞ = 48 mtorr. The centerline rotational temperature profiles for the isentropic "plug" flow and DSMC calculation startlines are shown in Figure 1. The isentropic startline gives a closer match to the data, but both calculations produce rotational temperatures higher than the data, even in the post-shock region. It should be pointed out that the gas rotational temperature is completely equilibrated to the translational temperature in the post shock region for all the simulations. Also shown in the figure is the result for a constant rotational collision number model using a value of 5 for that parameter. As was found in Reference 1, the constant collision number model predicts significantly different rotational temperatures than the variable rotational collision model, in a direction farther from the experimental data. Spatially extended calculations show that the post shock conditions slowly approach the chamber conditions over a distance of hundreds of orifice diameters downstream from the shock position. Because the DSMC calculation startline may still be problematic, the isentropic startline was used in all of the analyses reported here.

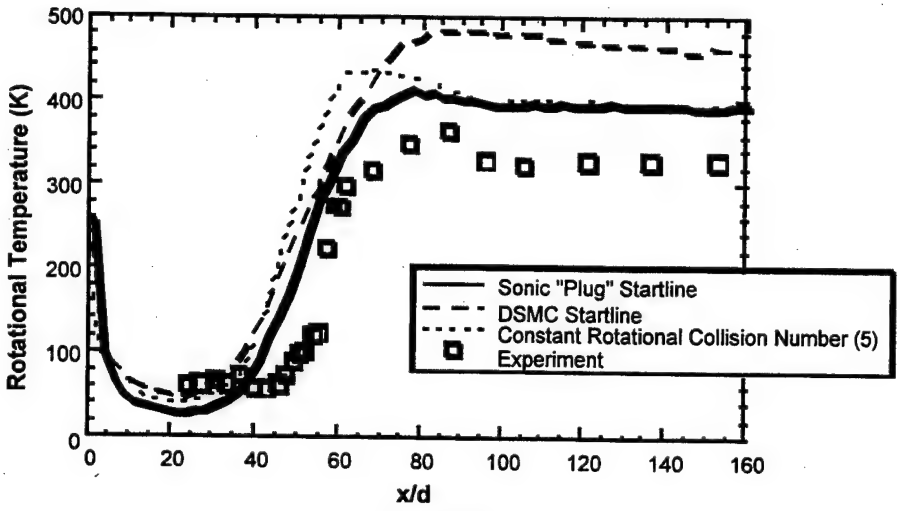

Figure 1
Effects of Startline and Collision Number

Different schemes were used to define the outflow boundary in the DSMC calculation. The boundary of the calculation was also placed at different distances downstream. It was found that, as long as the calculational region extended to about twice the distance to the shock, the boundary treatment and calculational boundary position did not affect the quantitative structure of the shock.

A portion of the expansion flow upstream of the shock attains translational temperatures below the 125 K level at which the Parker rotational relaxation model is known to be incorrect. In lieu of a full implementation of the Lebed' and Riabov[6] rotational relaxation model, a simplified scheme was used whereby the rotational relaxation collision number was set to a value of 10 for collisions in which the collisional energy was below an equivalent temperature of 125 K. From these results, it was demonstrated that the influence of the low temperature region

rotational relaxation process on the rotational temperatures in the shock region was negligible. A correction to the rotational relaxation model at low temperatures is therefore not necessary in comparing the predicted and measured rotational temperatures in the shock region.

To investigate the effects of changes in the calculational boundary conditions on the shock structure, a series of computations were made for a range of pressure ratios by varying the number density at the inflow startline and at the outflow vacuum chamber boundaries. The values of the parameters are shown in Table 2 and the results are shown in Figure 2. An increased pressure ratio (P_O/P) causes the shock position to move downstream as expected. The post shock rotational temperature is not affected significantly by the pressure ratio over the range investigated. The peak height of the rotational shock is not affected by the startline number density, but is dependent on the chamber density. The slope of the shock is also affected significantly by the chamber density. The significant change in the shock position with a small (10%) change in the startline number density points out the importance of an accurate startline for these conditions.

Table 2. Chamber and Startline Number Density Values

	Chamber Number Density (m^{-3})	Inflow Startline Number Density (m^{-3})
Baseline	1.556×10^{21}	2.858×10^{24}
Low Chamber	1.0×10^{21}	2.858×10^{24}
High Startline	1.556×10^{21}	3.1438×10^{24}

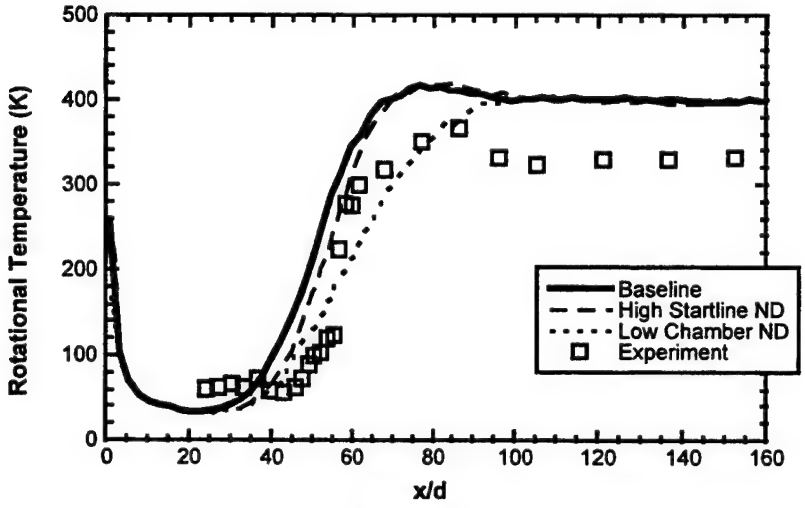

Figure 2
Effects of Pressure Ratio

To further understand the effects of the inflow startline on the predicted rotational temperature shock structure, two runs were made using inflow startline velocity and temperature 10% higher than the baseline values for the sonic "plug" startline. The results are shown in Figure 3. These small changes in inflow startline velocity and temperature produced a significant increase in the peak and post-shock rotational temperature and tended to flatten the profile. The rotational temperature shock position was moved downstream for the higher velocity case, but did not change for the higher temperature condition. Once again it is seen that small changes in

the inflow startline can produce significant changes in the predicted shock structure.

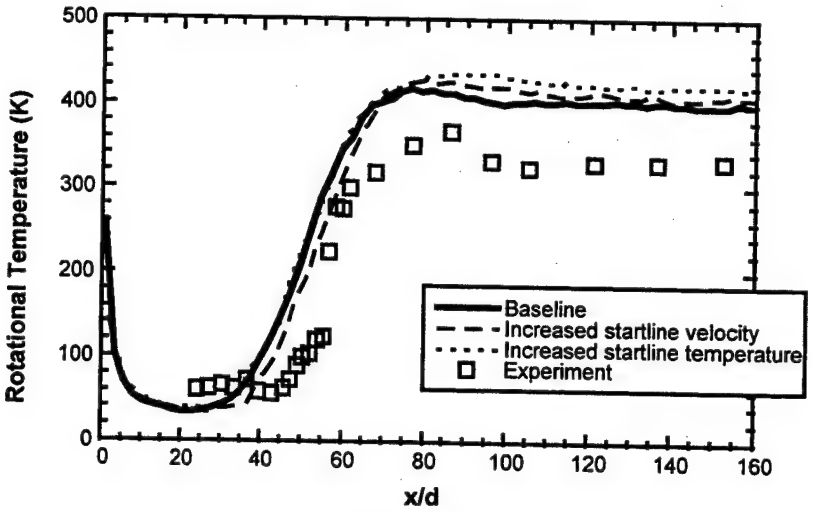

Figure 3
Effects of Startline Velocity and Temperature

CONCLUSIONS

The improvements to the DSMC rotational relaxation collision model implementation that have been made since the study in Reference 1 was completed have changed the predicted profiles of rotational temperatures in the expansion jet shock. When compared to the experimental data for Gochberg's Case 1,[2] the improvement is mixed. The position of the shock more closely matches the experimental results, but the peak height and post-shock temperature is now significantly greater than the data values.

For the low temperatures present in the initial part of the jet expansion, it is possible that the generalized hard sphere (GHS) collision model (Hassan and Hash[13]), which includes an attractive component of the molecular potential, may be more accurate than the repulsive power-law present in the VHS model. For example, in an equilibrium gas at T = 50 K, the GHS collision frequency is eight times the VHS value (using the GHS and VHS parameters given in Reference 14). This would tend to increase the equilibration of T_r to T_t in the expansion region. The GHS model was implemented using the rotational relaxation methods discussed in Hash, *et al.*,[14] and Choquet.[15] Because of a severe increase in computational time requirements for the collision selection procedures, it was not been possible to obtain solutions for this flow with the GHS model. As an alternative, the variable soft sphere (VSS) model (Koura and Matsumoto[16]) with the appropriate low temperature parameters has been considered but not yet implemented.

REFERENCES

1. Campbell, D.H., Wadsworth, D., and Gochberg, L.A., "DSMC Comparisons to Rotational Temperature Measurements in Jet Expansions with Finite Background Pressures," **Rarefied Gas Dynamics: Proceedings of the 19th International Symposium Held at the University of Oxford, 25-29 July 1994 (International Symposia)**, J. Harvey and G Lord, eds., Oxford: Oxford University Press, 1995, pp. 1300-1306.

2. Gochberg, L.A., *Rotational Nonequilibrium in Low Density Heated Free Jet Expansions of Nitrogen*, University of California at Berkeley, Ph. D. Thesis, 1993.

3. Gochberg, L.A., and Haas, B.L., "Rotational Relaxation Analysis for Nitrogen in Low-Density Freejet Expansions," **Rarefied Gas Dynamics: Proceedings of the 19th International Symposium Held at the University of Oxford, 25-29 July 1994 (International Symposia)**, J. Harvey and G Lord, eds., Oxford: Oxford University Press, 1995, pp. 476-82.

4. Gochberg, L.A., and Haas, B.L., "Evaluation of Rotational Relaxation Rate Models in Low-Density Expanding Flows of Nitrogen," AIAA Paper 95-2070, presented at the 30th AIAA Thermophysics Conference, San Diego, CA, Jun 19-22, 1995.

5. Parker, J.G., "Rotational and Vibrational Relaxation in Diatomic Gases," *Phys Fluids*, **2**, *4*, Jul-Aug 1959, pp. 449-62

6. Lebed', I.V., and Riabov, V.V., "Quantum Effects in Rotational Relaxation of a Freely Expanding Gas," *J Appl Mech and Tech Phys*, **20**, *1*, Jul 1979, pp. 1-3.

7. Murphy, H.R., and Miller, D.R., "Effects of Nozzle Geometry on Kinetics in Free-Jet Expansions," *J Phys Chem*, **88**, *20*, 27 Sep 1984, pp. 4474-8.

8. Campbell, D.H., "Direct Simulation Monte Carlo Analysis of the Near Field of Free Jets," AIAA Paper 89-1714, presented at the 24th AIAA Thermophysics Conference, Buffalo, NY, Jun 12-14, 1989.

9. Serikov, V.V., and Nanbu, N., "Methodological Aspects of MCDS Approach as Applied to 3-D Flow in the Sputtering Chamber," *Reports of the Inst of Fluid Science, Tohoku University,* **6**, 1994, pp. 43-72.

10. Boyd, I.D., "Rotational-Translational Energy-Transfer in Rarefied Non-Equilibrium Flows," *Phys Fluids A-Fluid Dynamics*, **2**, *3*, 1990, pp. 447-52.

11. Chung, C.H., Kim, S.C., Stubbs, R.M., and DeWitt, K.J., "DSMC and Continuum Analysis of Low-Density Nozzle Flow," AIAA Paper 93-0727, presented at the 31st AIAA Aerospace Sciences Meeting and Exhibit, Reno, NV, Jan 11-14, 1993.

12. Haas, B.L., Hash, D.B., Bird, G.A., Lumpkin, F.E. III, and Hassan, H.A., "Rates of Thermal Relaxation in Direct Simulation Monte Carlo Methods," *Phys Fluids*, **6**, *6*, Jun 1994, pp: 2191-201.

13. Hassan, H.A., and Hash, D.B., "A Generalized Hard Sphere Model for Monte Carlo Simulations," *Phys Fluids A-Fluid Dynamics*, **5**, *3*, Mar 1993, pp: 738-44.

14. Hash, D.B., Moss, J.N., and Hassan, H.A., "Direct Simulation of Diatomic Gases Using the Generalized Hard Sphere Model," *J Therm Heat Transfer*, **8**, *4*, Oct-Dec 1994, pp. 758-64.

15. Choquet, I., "Thermal Nonequilibrium Modeling Using the Direct Simulation Monte Carlo Method: Application to Rotational Energy," *Phys Fluids*, 6, *12*, Dec 1994, pp: 4042-53.

16. Koura, K., and Matsumoto, H., "Variable Soft Sphere Molecular Model for Inverse-Power-Law or Lennard-Jones Potential," *Phys Fluids A-Fluid Dynamics*, **3**, *10*, 1991, pp: 2459-65.

APPENDIX

DETAILS OF DSMC MODELS

APPENDIX

DSMC Collision Procedure

The basic Direct Simulation Monte Carlo (DSMC) methodology is well described in Bird.[1] The present study focused on the collision procedure, specifically the degree to which it can model certain types of nonequilibrium physics. The collision processes considered are summarized and consistent implementation of models into the DSMC algorithm is discussed, including key differences between the present approach and those in the literature.

Molecular Model

The present study was limited to atomic and diatomic species in the ground electronic state. For diatomic species, the internal modes (rotation and vibration) are nominally considered uncoupled, though some portions of this analysis could be applied to coupled states (including, e.g., quasi-bound rotational levels).

Rotational Mode. The rotational mode is described by a bounded version of the quantized rigid rotator model proposed by Boyd.[2] The rotational energy at level $j, 0 \leq j \leq j_D$, given by $\epsilon_r(j) = j(j+1)k\theta_r$, where θ_r is the characteristic rotational temperature (see, e.g., Bird,[1] Appendix A) and k is the Boltzmann constant. The maximum bound level is given by

$$j_D = \{-1 + [1 + (4D/k\theta_r)]^{1/2}\}/2 \tag{1}$$

where D is the dissociation energy (measured from the ground vibrational state).

The normalized equilibrium distribution of ϵ_r at temperature T is defined as

$$f'_B(j;T) = f_B(j;T)/Q_r(T) \tag{2}$$

$$f_B(j;T) = (2j+1)\exp(-\epsilon_r/kT) \tag{3}$$

$$Q_r(T) = \sum_{j=0}^{j=j_D} f_B(j;T) \tag{4}$$

Replacing the sum in the partition function Q_r by integration gives

$$f'_B(j;T) \sim \frac{\theta_r}{T}(2j+1)\frac{\exp(-\epsilon_r/kT)}{1-\exp(-D/kT)} \tag{5}$$

This reduces to Equation (2) of Boyd for the case $kT \ll D$. Initial rotational energies for particles are defined by sampling from this distribution.

The code outputs a rotational temperature calculated from the sampled average energy $\bar{\epsilon}_r$ by assuming the equilibrium distribution of Equation (3) and solving for the parameter T_r in

$$\bar{\epsilon}_r = \frac{\sum_{j=0}^{j=j_D} \epsilon_r f_B(j;T_r)}{Q_r(T_r)} \tag{6}$$

It should be noted that the rotational distribution function represented by diatoms in the simulation need not be equilibrium, and this temperature should be interpreted as simply an estimate of the average energy present in the rotational mode.

Vibrational Mode. The vibrational mode is described by the bound quantized anharmonic oscillator model of Bergemann and Boyd.[3] Bound vibrational energy levels $v, 0 \leq v \leq v_D$, of energy $\epsilon_v(v)$ are nominally generated from the Dunham expansion using the spectroscopic constants available in Huber & Herzberg.[4] (Note: the zero point energy was subtracted to obtain $\epsilon_v(0) = 0$).

The normalized equilibrium distribution of ϵ_v at temperature T is defined as

$$f'_B(v;T) = f_B(v;T)/Q_v(T) \quad (7)$$

$$f_B(v;T) = \exp\left(-\epsilon_v/kT\right) \quad (8)$$

$$Q_v(T) = \sum_{v=0}^{v=v_D} f_B(v;T) \quad (9)$$

Initial vibrational energies for particles are defined by sampling from this distribution. Note that for anharmonic levels, the inversion of the distribution function to assign particle vibrational energy as used by Bird[1] (Appendix C, and implemented in the sample programs) is not valid and will result in incorrect distributions (with the error increasing with T). That method is valid, however, for harmonic oscillators (constant energy gap $\epsilon_v(v) = vk\theta_v$).

The code outputs a vibrational temperature T_v calculated from the sampled energy $\bar{\epsilon}_v$ analogously to that for T_r.

Collision Procedure

The collision procedure is based on the serial redistribution method of Bird[1] (Chap. 5.5), as extended by Haas, et al.[5] A schematic of the basic procedure is given in Figure A1. The number of pair selections per time step under the No Time Counter (NTC) model (Bird,[1] Chap. 11.2), is based on the maximum value of the product of the elastic cross section $\sigma_{el}(\epsilon_t)$ (here given by the Variable Hard Sphere (VHS) model), and the relative speed g defined by the relative translational energy $\epsilon_t = m_r g^2/2, m_r$ being the reduced mass of the collision pair, and will thus recover the elastic relaxation rate. Collision pairs are randomly selected and are then accepted with the probability $P = \sigma_{el} g/(\sigma_{el} g)_{max}$ by comparing P with a uniform random number $R, 0 < R < 1$. The code allows for the species to be combined into 'groups' (Bird,[1] Chap 11.2), with a $(\sigma_{el} g)_{max}$ stored for each, to improve acceptance efficiency for cases where large disparities between nominal σ_{el} or g arise between species.

Details of Collision Events. All accepted collision pairs undergo redistribution of translational energy as the last process of the collision procedure. The available inelastic or chemical reaction collision events are dependent on the type of the species pair selected. For atom-atom collisions, only a recombination reaction is potentially available. For diatom-atom collisions, a dissociation and, possibly, an exchange reaction, along with vibrational-translational (V-T) and rotational-translational (R-T) relaxation, are available. Diatom-diatom collisions are similar to those for diatom-atom pairs; however, the exchange reaction

is not available. Figure A2 shows the process by which possible collision outcomes are modeled for the case of a diatom-diatom pair, denoted A_2–B_2, which has been accepted for collision via the logic of Figure A1. The figure shows only the case where the first particle chosen for testing is A_2. The case for B_2 chosen first is completely analogous. Note that the diatoms need not be homomolecular.

The serial procedure includes the 'particle selection prohibiting multiple relaxation' logic of Haas, et al.[5] to calculate the probability of each event. This method is an attempt to improve the numerical treatment of, rather than the physical modeling of, several dependent collision processes. The logic analytically relates the molecular probability P_x of a relaxation event of mode x and the macroscopic average value (typically described by the input collision number Z_x) under equilibrium conditions. The collision number is defined as ratio of the mode x relaxation time to an elastic collision time, $Z_x \sim \tau_x/\tau_c$, so approximately $P_x \sim 1/Z_x$. The Bird serial NTC methodology determines the total number of collisions from the elastic cross section. The Haas, et al.[5] logic increases the probabilities for inelastic events ($P > 1/Z$) to obtain the proper relaxation rate (characterized by Z) of each mode. Using this approach, the event cross section $\sigma_x \sim P_x \sigma_{el}$ can be identified. Note the requirement that a microscopic probability P or cross section σ_x be related to (ill-defined) macroscopic quantities such as Z is a common weakness of the majority of DSMC collision models.

In the present study, the Haas, et al.[5] logic has been applied only to the internal relaxation (vibration followed by rotation) portion of the complete serial procedure of Figure A2. The formulae for the P are dependent on the ordering of modes in the serial procedure (see, e.g., Appendix B of Haas, et al.). For the case of vibrational relaxation in the diatom-diatom collision of Figure A2, each probability is dependent on the relaxation rate values of both of the colliding species, and the P_{v_2} of the second diatom (B_2 in Figure A2) is dependent on the value calculated for the first diatom A_2 tested (but not accepted) P_{v_1}:

$$P_{v_1} = \text{root of} [P_{v_1}^2 + (X_2 - X_1 - 2)P_{v_1} + 2X_1 = 0] \tag{10}$$

$$P_{v_2} = \frac{X_2}{(1 - P_{v_1}/2)} \tag{11}$$

where

$$X_1 = \left(\frac{\zeta_t + \zeta_v}{\zeta_t} \frac{1}{Z_v} \right)_1 \tag{12}$$

with all quantities in X_1 those for impact of species 2 on target diatom 1, and similarly for X_2. The values of Z are as discussed below. The ζ terms describe the degrees of freedom of the energy modes of the diatoms appearing in the Borgnakke-Larsen procedure. The translational collision energy mode (biased by the NTC collision selection) term is $\zeta_t = 5 - 2\omega_B$ and the vibrational energy mode term $\zeta_v = \zeta_v(T_v) = 2\bar{\epsilon}_v/(kT_v)$ (Equation (11.28) of Bird), based on the sampled cell vibrational temperature of the target species. As shown in Figure A2, in the serial (or particle) approach prohibiting multiple relaxation, only the first accepted relaxation event is carried out. For example, if $R < P_{v_1}$, then the post-collision vibrational level v' of A_2 is calculated, the remaining energy $\epsilon_c - \epsilon'_v$ is

redistributed into the translational energy (i.e., velocities) of the colliding pair, and the collision is concluded. Otherwise the next test ($R < P_{v_2}$) is made.

Since the tests for rotational relaxation follow those for vibrational relaxation, the rotational relaxation probabilities P_{r_1}, P_{r_2} become dependent on those for vibration

$$P_{r_1} = \text{root of}[P_{r_1}^2 - (2 - Y_2/P_v + Y_1/P_v)P_{r_1} + 2Y_1/P_v = 0] \quad (13)$$

$$P_{r_2} = \frac{Y_2}{(1 - P_{r_1}/2)P_v} \quad (14)$$

$$P_v = (1 - P_{v_1})(1 - P_{v_2}) \quad (15)$$

where, analogous to the vibration case

$$Y_1 = \left(\frac{\zeta_t + \zeta_r}{\zeta_t}\frac{1}{Z_r}\right)_1 \quad (16)$$

and the rotational mode contributes $\zeta_r = 2$.

These formulae place additional mathematical bounds (which may or may not have a physical basis) on the allowable Z. In contrast to the discussion in the paper of Haas, et al.,[5] the method has been found here to be valid only for the case of near-constant Z and will not accomodate coupled processes for which each possesses a $Z_x(\epsilon_c)$. Also, note that inclusion of additional serial collision events (e.g., as shown in Figure A2, the dissociation test precedes vibration) means that the coupling between processes becomes excessively complex, and this method does not appear feasible for general application. The null collision selection method of Koura[6] is less mathematically precise, but is more easily generalizable and more physically consistent. It appears that method will be useful in future studies, but will not be discussed further here.

Cross Sections and Probabilities. Elastic Cross Sections. Elastic (and thus for the nominal Bird method, total) cross sections are based on VHS values

$$\sigma_{el}(g) = \sigma_{ref}\epsilon_t^{-\omega_B+1/2} \quad (17)$$

using the (constant) reference cross section (σ_{ref}) and exponents in the viscosity temperature relationship ($\mu(T) \sim T^{\omega_B}$) tabulated in, e.g., Bird,[1] Appendix A. Using the general Borgnakke-Larsen procedure, only some fraction ($\sim 1/Z_x$) of collision pairs accepted for elastic collisions are tested for chemical reaction or inelastic relaxation events.

Rotational Relaxation. Models for rotational (specifically rotational-translational or R-T) relaxation are generally not sophisticated at the present time. All available DSMC models apparently are based on the theoretical model given by Equation (45) of Parker,[7] which predicts qualitatively the experimentally observed temperature dependence of the macroscopic rotational collision number $Z_r(T)$. Boyd[2] (see also Choquet[8] and Koura[9]) have generalized this to an energy-dependent form $Z_r(\epsilon_c)$ for use in DSMC which reproduces the Parker temperature dependence under equilibrium.

Relatively little modeling of R-T relaxation was done using the present DSMC code in this part of the effort. For cases where only rotational relaxation has been allowed in the serial procedure, the energy-dependent form $Z_r(\epsilon_c)$ given by Equation (24) of Choquet[8] (rewritten for Z_r) has been used

$$Z_r(\epsilon_c) = \frac{Z_r^\infty}{1 + 4\pi/3\,(kT^*/\epsilon_c)^{1/2} + (\pi^2/4 + 2)(kT^*/\epsilon_c)} \tag{18}$$

(note the slight difference in the final constant term in the denominator, chosen to match the VHS form given by Equation (18) of Hash, et al.[10]).

For cases where rotational relaxation was preceded by the test for vibrational relaxation, the temperature-dependent model $Z_r(T)$ based on the VHS form given by Equation (18) of Hash, et al.[10] (see also Equation (21) of Choquet[8]) has been used

$$Z_r(T) = Z_r^\infty \frac{\Gamma(3 - \omega_B)}{\Gamma(3 - \omega_B) + 4\pi/3\,\Gamma(5/2 - \omega_B)(T^*/T)^{1/2} + 2(\pi^2/4 + 2)\Gamma(2 - \omega_B)(T^*/T)} \tag{19}$$

where $\Gamma()$ is the gamma function, T is the directly sampled translational temperature in the cell in which the collision partners reside, and T^*, Z_r^∞ are as given in, e.g., Parker.[7]

Note that using the serial method and the R-T model here, only a single particle of the selected pair is allowed to relax per collision event. Consideration of the possibility of a rotational-rotational (R-R) event during a diatom-diatom collision would require the incorporation of relatively complex pairwise probabilities such as those given by Equation (26) of Koura.[9]

Vibrational Relaxation. Several models of vibrational-translational (V-T) relaxation, of varying levels of mathematical and physical sophistication, were implemented. Relatively comprehensive comparisons of these V-T models were made and are documented as part of this report.

1. $Z_v(T)$ based on the Millikan & White (M&W) correlation,[11] $\tau_v = \exp\left(AT^{-1/3} + B\right)/(nkT)$, where n is the number density, T is the cell translational temperature, and the input constants A and B are available from the original report and subsequent compilations (see, e.g., Moreau[12]).

2. The M&W value including the empirical Park[13] correction factor which limits the minimum allowable τ_v (and thus Z_v), $Z_v(T) = (\tau_v + \tau_{park})/\tau_c$, where τ_{park} is some constant C or $C(T) > \tau_c$, as discussed in Park. The correction factor is of non-negligible magnitude only for relatively high temperatures and was not found to be important in the present work. However, by fitting results to the more sophisticated models discussed below, improved correction factors can be generated.

3. The Bird[1] (Chap 11.4) form of the M&W model, where $Z_v(T_c)$ is calculated based on a temperature corresponding to the collision energy, $T_c = \epsilon_c/(\zeta_t + \zeta_v)k$. This model,

using the M&W rates corresponding to T_c, results in vibrational collision numbers Z_v one or more orders of magnitude too small (Choquet[14]) and thus leads to excessive relaxation rates. This error can be seen clearly in the stagnation streamline flowfield of Figure 12.47 of Bird. Those calculations use the serial procedure, similar to that shown in Figure A2 here, but do not use the logic of Haas, et al.[5] The small value of Z_v means the majority of collisions undergo vibrational relaxation, and relatively few are tested for rotational relaxation. This gives rise to the non-physical behavior seen in that figure that $T_v > T_r$ through the shock layer.

4. The Abe[15] single-quantum-jump harmonic oscillator model valid for low temperatures, calibrated to reproduce the M&W relaxation rate

$$P_{v,v-1} = vP_{10} \tag{20}$$

$$P_{v,v+1} = (v+1)P_{10}\left(\frac{\epsilon_t - k\theta_v}{\epsilon_t}\right)^{3/2-\omega_B}, \quad (\epsilon_t > k\theta_v) \tag{21}$$

P_{10} is a constant probability related to the rate constant k_{10} for $(v, v') = (1, 0)$ transitions from the M&W correlation (see also Koura[6])

$$k_{10} = \frac{1}{[1-\exp(-\theta_v/T)]\tau_v} = \int_0^\infty P_{10}\sigma_{el}gf(g)dg = \Gamma(5/2-\omega_B)P_{10}/2 \tag{22}$$

The net probability of vibrational relaxation is $P_v = P_{v,v-1} + P_{v,v+1}$. Note the formulae given by Equation (23) and (24) of Abe assume hard sphere collision mechanics. The formulae here are generalized to the VHS model (and use the present notation $\omega_B = \omega_{(\text{Abe})} + 1/2$, and the rate constant $k_{10} = k_{1,0(\text{Abe})}/n$). For a hard sphere, Abe's Equation (24) should read $k_{1,0} = nP_{10}\sigma_{ref}[2kT/(\pi m_r)]^{1/2}$; his χ is extraneous.

5. The energy-dependent version of the Abe model given by Equation (22) of Abe and the related Equations (20) and (21) of Boyd,[16] e.g.,

$$P_{v,v+1} = C(v+1)\frac{(g')^{5+2\omega}}{g^2}\exp(-g^*/g') \tag{23}$$

where C and g^* are constants and the post-collision relative speed is defined by $\epsilon_t' = m_r(g')^2/2 = \epsilon_t - k\theta_v$.

As discussed by Choquet,[14] these formulations lead to difficulties with equipartition of energy and were not pursued further.

6. The Koura[6] form of the Heidrich, et al.[17] improvement to forced oscillator, impulsive transfer semiclassical (ITFITS) multi-quanta-jump harmonic oscillator model, valid for diatom-atom collisions over a wide range of temperatures. The form given in Koura apparently uses a non-standard polynomial function, and for clarity Equation (23) of the original reference is used

$$P_{v,v'} = v!v'!(\langle\Delta E\rangle)^{v+v'}\exp(-\langle\Delta E\rangle)\left(\sum_{l=0}^{min(v,v')}\frac{(\langle\Delta E\rangle)^{-l}}{l!(v-l)!(v'-l)!}\right)^2 \tag{24}$$

and the symmetrized energy gap term $\langle \Delta E \rangle$) is as defined in Equation (22) of that reference. The total probability of vibrational relaxation is given by $P_v = \sum_{v'} P_{v,v'}$. Note that versions of the ITFITS model applicable to anharmonic oscillators[18] and diatom-diatom collision partners[19] are available, along with a similar semiclassical model for V-V[20] transfer, but have not yet been implemented.

Dissociation. Relatively few models of dissociation are available which incorporate any degree of physical realism. It is expected that models which incorporate an (adjustable) degree of favoring of vibrational energy would be more realistic. Several models have been implemented and analyzed in this report. All models allow dissociation (with probability P_D) only of a diatom with the collision energy $\epsilon_c = \epsilon_t + \epsilon_r + \epsilon_v > D$. ($P_D = 0$ for a diatom with insufficient collision energy for this endothermic reaction). All models need to be calibrated to some known equilibrium rate constant at some temperature (or some range of temperatures). As with any other calibration to some macroscopic property, the calibration constant will be dependent on the details of the collision procedure. Relatively comprehensive comparisons of these dissociation models have been made and are documented as part of this report.

1. The Exact Available Energy (EAE) model of Bird[1] (Chap 6.7, 11.5, see also Carlson & Bird[21]), where dissociation is modeled using the Borgnakke-Larsen redistribution of vibrational energy, and a diatom dissociates when the accepted post-collision vibrational energy $v' > v_D$. The model requires no input parameters, but a calibration constant is allowed for.

2. A form of the Weak Vibrational Bias (WVB) model, given by Equation (22) of Koura[6]

$$P_D = A_i \left[1 - \frac{D - \epsilon_v}{\epsilon_t}\right] \exp\left(\lambda[\frac{\epsilon_v}{D} - 1]\right) \tag{25}$$

   where A_i is a calibration constant chosen to allow adjustment of the overall rate constant, and λ is an input parameter controlling the degree of vibrational favoring or weighting. The symmetrized cross section present in the original form has been omitted due to its small effect.

3. The Full Threshold (FT) model of Macheret, et al.[22] The model characteristics and appropriate probabilities, Equations (6), (10) and (16)-(19) of that reference, are well described in that report and are not repeated here. The model contains no adjustable parameters, but a calibration constant A_i has been added here.

4. The Simplified Threshold (ST) model of Boyd,[23] based on the FT model, but using simplified forms of the probability equations (Equations (25) and (30) in Macheret, et al., Equations (4)-(9) in Boyd), valid only for the limiting case of high translational energy collisions, $\epsilon_t \gg D$.

Exchange. The choice of the model for exchange is dependent on the assumed degree of vibrational favoring present in the reaction. As shown in this report, the dominant exchange reactions in air, the Zeldovich reactions, are not (or are only weakly) vibrationally favored. As such, the EAE model as described by Bird[1] (Chap 6.8) has been found to be suitable for describing the forward (endothermic) reaction (in the sense of recovering the vibrational distribution of diatoms chosen to undergo exchange, and in recovering the approximate Arrhenius equilibrium rate constant). This model is implemented analogously to that for dissociation, with a diatom possessing $\epsilon_c = \epsilon_t + \epsilon_r + \epsilon_v > E_a$, ($E_a$ being the activation energy) undergoing exchange when the sampled post-collision vibration level $v' > v_{E_a}$.

Relatively little analysis of the combined forward / reverse reaction chemistry model has been done here. Following the logic of Bird, the (potentially temperature-dependent) reverse reaction probability can be evaluated using the equilibrium rate constant and the calibrated form of the forward analytic EAE rate constant, evaluated at the cell temperature.

Recombination. For the low gas densities of interest, recombination reactions (dependent on three-body collisions) are negligible. As such, relatively little analysis of recombination models has been done here. Models of varying degrees of physical validity can be generated using the principle of detailed balance and the dissociation models described above.

To calibrate the combined dissociation / recombination models to some known equilibrium rate (or degree of dissociation), limited calculations have been done using the simple temperature-dependent recombination model of Bird[1] (Chap 6.7, 11.5), based on the analytic EAE dissociation rate constant. Since the effective rate constant extracted from the simulations was found to be different from that predicted analytically, the recombination probability must be recalibrated to recover expected the equilibrium constant over some range of temperature.

Post-Collision Redistribution of Energy. A particle that passes the acceptance / rejection test (i.e., $R < P_x$, where R is a uniform random number) shown in Figure A2 undergoes redistribution of energy in that mode x (for the case of internal relaxation) or undergoes reaction (for the case of chemical reaction). For the case of internal relaxation, for most of the collision models considered here, the redistribution is done via the generalized Borgnakke-Larsen procedure (Bird,[1] Chap. 5.5), where the post-collision value is sampled from the Borgnakke-Larsen (equilibrium) distribution at the collision energy $\epsilon_c = \epsilon_t + \epsilon_x$, where ϵ_t denotes the relative translational energy and ϵ_x denotes the energy in mode x of the particle undergoing redistribution.

Rotation. Given a rotationally inelastic collision, the post-collision rotational level j' is sampled using a modified version of the Boyd[2] Borgnakke-Larsen method. The peak-normalized distribution is given by Equation (10) of Boyd as

$$g'(j';\epsilon_c) = \frac{(2j'+1)[\epsilon_c - j'(j'+1)k\theta_r]^{1-\omega}}{(2j_p+1)[\epsilon_c - j_p(j_p+1)k\theta_r]^{1-\omega}} \tag{26}$$

where the notation of Boyd is retained for $\omega(=\omega_B - 1/2)$, and the peak occurs at

$$j_p = \left(-1 + \left[\frac{1 + 4\epsilon_c/k\theta_r}{3 - 2\omega}\right]^{1/2}\right)/2 \tag{27}$$

This equation differs from that given by Equation (11) of Boyd. It is, however, analogous to that given by Equation (30) of Koura[9] for the case of pair, rather than single particle, relaxation. The maximum allowable post-collision j_{max} is limited to j_D if $\epsilon_c > D$; otherwise it is as given by Equation (12) of Boyd (the present Equation (1), with D replaced by ϵ_c). Comparing j_{max} and j_p, since $\epsilon_c \geq \epsilon_r$, the relation $j_{max} \geq j_p$ will always be satisfied, and the requirement of item (3) of Boyd is irrelevant. Note that in this method, the post-collision value j' is allowed to take any value $0 \leq j' \leq j_{max}$, including $j' = j$, and also that there is no restriction that $\delta_j = |j - j'|$ be even-valued for homonuclear molecules. These constraints could be implemented numerically, however. More analysis of rotational relaxation will be carried out in the future.

Vibration. The present analysis includes only V-T processes and ignores the physically-allowed vibrational-vibrational (V-V) relaxation process in diatom-diatom collisions. For the Abe state-specific single-quantum model, the post-collision vibrational level is determined directly by acceptance (or rejection) of $P_{v+1} = P_{v,v+1}/P_v$ (or $P_{v-1} = 1 - P_{v+1}$). A similar method is used for the Koura ITFITS formulation (though a single state must be probabilistically chosen from the multiple-quanta available).

For the other models, v' is chosen by sampling from the Borgnakke-Larsen distribution as discussed by Bird[1] (Chap. 5.6), where $0 \leq v' \leq v_{max}$, with $\epsilon_v(v_{max}) \leq \epsilon_c$. Note that these models allow $v' = v$.

Dissociation. When a dissociation reaction occurs, the dissociation energy is decremented from the collision energy $\epsilon_c = \epsilon_t + \epsilon_r + \epsilon_v$ of the dissociating diatom, and the remaining energy is redistributed to the relative translational energy of the colliding pair, and then to the relative translational energy of the dissociating atoms following the method of Bird[1] (Chap 11.5).

Exchange. When an exchange reaction occurs, the heat of reaction is decremented from the collision energy $\epsilon_c = \epsilon_t + \epsilon_r + \epsilon_v$ of the colliding diatom, and the remaining energy is serially redistributed to the vibrational and rotational mode of the newly-created diatom, and then to the relative translational energy of the new diatom-atom pair.

Recombination. Following the Bird[1] (Chap 11.5) EAE model, the new diatom is created with velocity equal to the center of mass velocity of the recombining pair, a random third body is chosen for collision with the new diatom, and the energy $\epsilon_t + D$ is redistributed serially into the vibrational and rotational modes of the newly-created diatom, and then to the relative translational energy of the diatom-third body pair.

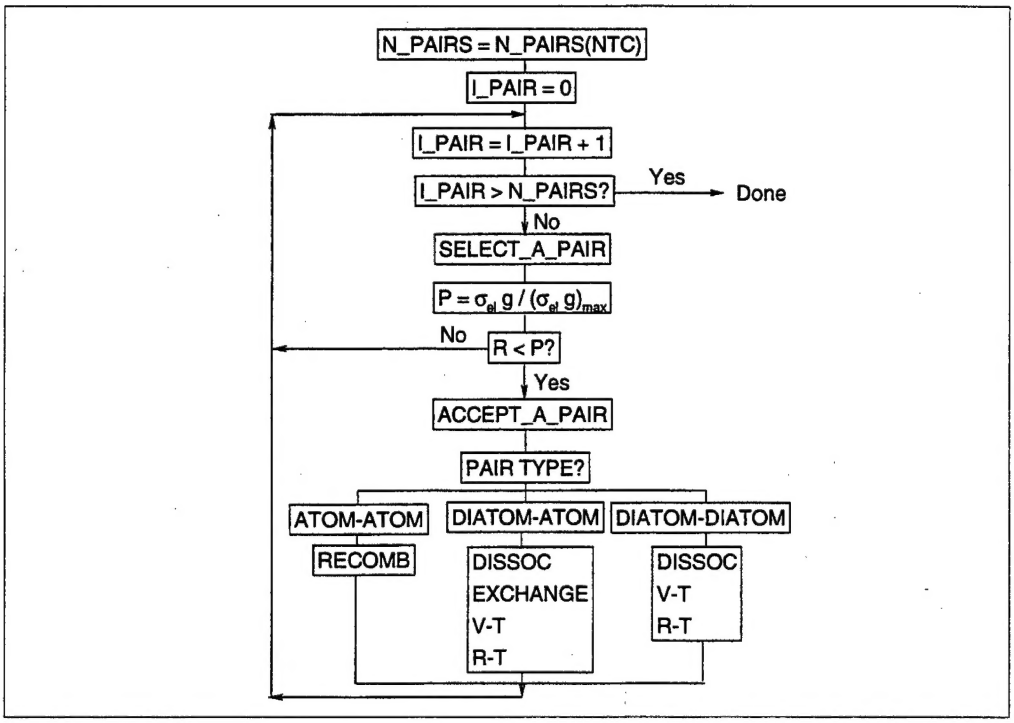

Figure A1
Schematic of Serial Collision Procedure.

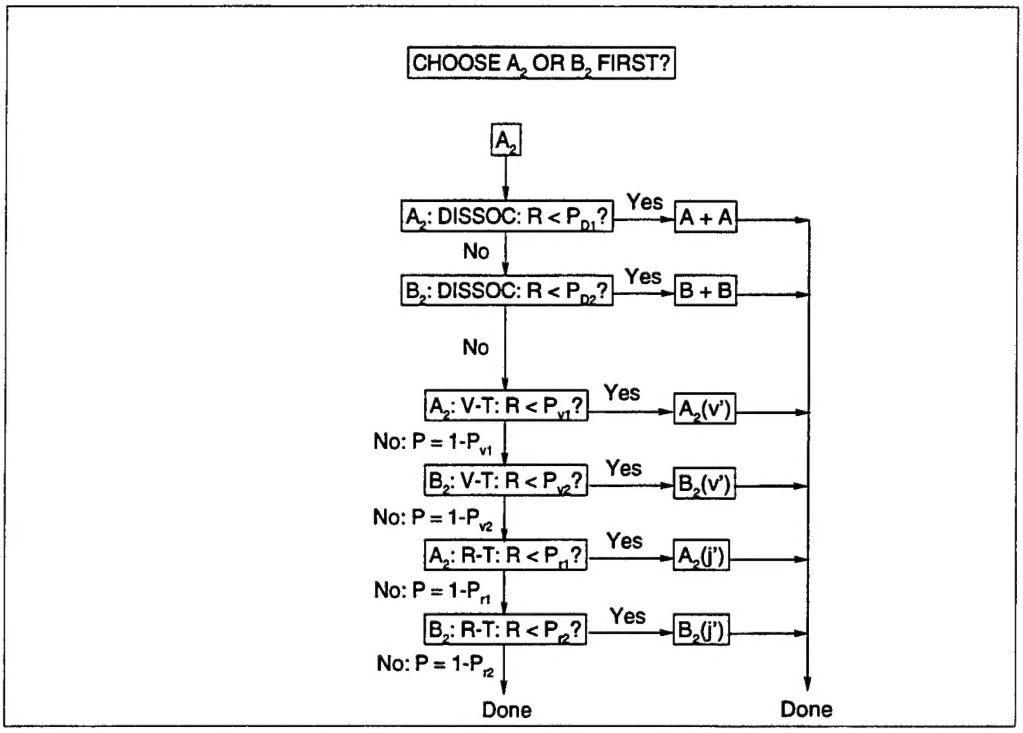

Figure A2
Schematic of Inelastic or Chemical Reaction Collision Event Selection Procedure for Diatom-Diatom Pair, with Diatom A_2 chosen first (B_2 analogous).

References

[1]Bird, G. A., **Molecular Gas Dynamics and the Direct Simulation of Gas Flows** Clarendon Press, Oxford, 1994

[2]Boyd, I. D., "Relaxation of discrete rotational energy distributions using a Monte Carlo method," *Phys. Fluids A* **5**, 9, May 1993 pp. 2278–2286.

[3]Bergemann, F. and Boyd, I. D., "New discrete vibrational energy model for direct simulation Monte Carlo method," in **Rarefied Gas Dynamics: Experimental Techniques and Physical Systems**, edited by Shizgal, B. D. and Weaver, D. P., AIAA, Washington, D.C., 1994, pp. 174–183.

[4]Huber, K. P. and Herzberg, G. **Molecular Spectra and Molecular Structure IV. Constants of Diatomic Molecules**, Van Nostrand Reinhold, New York, 1979

[5]Haas, B. L., Hash, D. B., Bird, G. A., Lumpkin, F. E., Hassan, H. A. "Rates of thermal relaxation in direct simulation Monte Carlo methods," *Phys. Fluids* **6**, 6, Jun 1994 pp. 2191–2201.

[6]Koura, K. "A set of model cross sections for the Monte Carlo simulation of rarefied real gases: Atom-diatom collisions," *Phys. Fluids* **6**, 10, Oct 1994 pp. 3473–3486.

[7]Parker, J. G., "Rotational and vibrational relaxation in diatomic gases," *Phys. Fluids* **2**, 4, Jul 1959 pp. 449–462.

[8]Choquet, I., "Thermal nonequilibrium modeling using the direct simulation Monte Carlo method: Application to rotational energy," *Phys. Fluids* **6**, 12, Dec 1994 pp. 4042–4053.

[9]Koura, K., "Statistical inelastic cross-section model for the Monte Carlo simulation of molecules with discrete internal energy," *Phys. Fluids A* **4**, 8, Aug 1992 pp. 1782–1788.

[10]Hash, D. B. and Hassan, H. A., "Direct simulation with vibration-dissociation coupling," *J. Thermophys. and Heat Transfer* **7**, 4, Oct 1993 pp. 680–686.

[11]Millikan, R. C. and White, D. R., "Systematics of vibrational relaxation," *J. Chem. Phys.* **39**, 12, Dec 1963 pp. 3209–3213.

[12]Moreau, S., *Computation of High-Altitude Hypersonic Flow-Field Radiation*, Ph.D. dissertation, Stanford University, Stanford, California, 1994.

[13]Park, C., **Nonequilibrium Hypersonic Aerothermodynamics**, Wiley & Sons, New York, 1988

[14]Choquet, I., "Vibrational nonequilibrium modeling using direct simulation part 1: Continuous internal energy," *J. Thermophys. and Heat Transfer* **9**, 3, Jul 1995 pp. 446–455.

[15]Abe, T., "Inelastic collision model for vibrational-translational and vibrational-vibrational energy transfer in the direct simulation Monte Carlo method," *Phys. Fluids* **6**, 9, Sep 1994 pp. 3175–3179.

[16]Boyd, I. D., "Analysis of vibrational-translational energy transfer using the direct simulation Monte Carlo method," *Phys. Fluids A* **3**, 7, Jul 1991 pp. 1785–1791.

[17]Heidrich, F. E., Wilson, K. R., and Rapp, D., "Collinear collisions of an atom and harmonic oscillator," *J. Chem. Phys.* **54**, 9, May 1971 pp. 3885-3897.

[18]Morse, R. I. and LaBrecque, R. J., "Collinear collisions of an atom and a morse oscillator: An approximate semiclassical approach," *J. Chem. Phys.* **55**, 4, Aug 1971 pp. 1522–1530.

[19]Morse, R. I., "Semiclassical transition probabilities for collinear diatom-diatom collisions," *J. Chem. Phys.*, **56**, 5, Mar 1972 pp. 2329-2332.

[20]Rapp D., and Englander-Golden, P., "Resonant and near-resonant vibrational-vibrational energy transfer between molecules in collisions," *J. Chem. Phys.*, **40**, 2, Jan 1964 pp. 573–575.

[21]Carlson, A. B. and Bird, G. A., "Implementation of a vibrationally linked chemical reaction model for DSMC," in **Rarefied Gas Dynamics, Proceedings of the 19th International Symposium, Oxford 1994**, edited by Harvey, J. and Lord, G., Oxford University Press, Oxford, 1995, pp. 434–440

[22]Macheret, S. O., Fridman, A. A., Adamovich, I. V., Rich, J. W., and Treanor, C. E., "Mechanisms of nonequilibrium dissociation of diatomic molecules," AIAA Paper 94-1984, Jun 1994.

[23]Boyd, I. D., "A threshold line model for the direct simulation Monte Carlo method," *Phys. Fluids* **8**, 5, May 1996, pp. 1293-1300.